



Understanding the Neutron Star Population with the SKAO Telescopes

L. Levin¹, M. Bagchi^{2,3}, M. Burgay⁴, A. T. Deller⁵, V. Graber⁶, A. Igoshev⁷,
M. Kramer^{8,1}, D. Lorimer⁹, B. Posselt¹⁰, T. Prabu¹¹, K. Rajwade¹⁰, N. Rea^{12,13},
B. Stappers¹, T. M. Tauris^{14,8}, P. Weltevrede¹ and the SKAO Pulsar Science
Working Group

¹*Jodrell Bank Centre for Astrophysics, Department of Physics and Astronomy, The University of Manchester, Manchester M13 9PL, UK*

²*The Institute of Mathematical Sciences, Taramani, Chennai 600113, India*

³*Homi Bhabha National Institute, Training School Complex, Anushakti Nagar, Mumbai 400094, India*

⁴*INAF – Osservatorio Astronomico di Cagliari, Via della Scienza 5, I-09047 Selargius, (CA), Italy*

⁵*Centre for Astrophysics and Supercomputing, Swinburne University of Technology, Hawthorn, VIC 3122, Australia*

⁶*Department of Physics, Royal Holloway, University of London, Egham, TW20 0EX, UK*

⁷*School of Mathematics, Statistics and Physics, Newcastle University, Newcastle upon Tyne, NE1 7RU, UK*

⁸*Max-Planck-Institut für Radioastronomie, Auf dem Hügel 69, D-53121 Bonn, Germany*

⁹*Department of Physics and Astronomy, West Virginia University, Morgantown, WV 26506-6315, USA*

¹⁰*Department of Astrophysics, University of Oxford, Denys Wilkinson Building, Keble Road, Oxford, OX1 3RH, UK*

¹¹*Raman Research Institute, Bangalore, India*

¹²*Institute of Space Sciences (ICE-CSIC), Campus UAB, C/ de Can Magrans s/n, Cerdanyola del Vallès (Barcelona) 08193, Spain*

¹³*Institut d'Estudis Espacials de Catalunya (IEEC), Castelldefels, Spain*

¹⁴*Department of Materials and Production, Aalborg University, Fibigerstræde 16, 9220 Aalborg, Denmark*

E-mail: Lina.Preston@manchester.ac.uk

The known population of non-accreting neutron stars is ever growing and currently consists of more than 3500 sources. Pulsar surveys with the SKAO telescopes will greatly increase the known population, adding radio pulsars to every subgroup in the radio-loud neutron star family. These discoveries will not only add to the current understanding of neutron star physics by increasing the known sample, but will undoubtedly also uncover new types of sources that will challenge our theories of a wide range of physical phenomena. A broad variety of scientific studies will be made possible by a significantly increased population of neutron stars, unravelling questions such as: How do isolated pulsars evolve with time; What is the connection between magnetars, high B-field pulsars, and the newly discovered long-period pulsars; How is a pulsar's spin-down related to its radio emission; What is the nuclear equation of state? Increasing the numbers of pulsars in binary systems enables both larger numbers and higher precision tests of gravitational theories and general relativity, as well as probing the neutron star mass distribution. The excellent sensitivity of the SKAO telescopes combined with the wide field of view, large numbers of simultaneous tied-array beams that will be searched in real time, wide range of observing frequencies, and the ability to form multiple sub-arrays will make the SKAO an excellent facility for neutron star research. This chapter presents an overview of different types of neutron stars and discusses how the SKAO will aid in our understanding of the neutron star population.

1 Introduction

The known population of neutron stars (NSs) has increased quickly over the last decade with the completion of new, more sensitive telescopes, such as the FAST and the MeerKAT radio telescopes, and is currently standing at over 3500 sources¹. The population is surprisingly diverse, with different subgroups exhibiting a variety of characteristics. The sources span many orders of magnitude in spin period (P) and period derivative (\dot{P}), and hence also in inferred magnetic field strength and characteristic age, as shown in the $P - \dot{P}$ diagram in Figure 1. The different NS subgroups, to some extent, show different radio emission properties in terms of e.g. spectra, emission modes, variability, and intermittency, indicating different magnetospheric conditions (Oswald et al., 2026). One of the important outstanding questions in the field of NS research is, if, and how all the varied subgroups fit together into one unified NS family.

In this chapter, we describe the different subgroups of NSs, give an overview of the current state of the field, and discuss how observations with the SKAO telescopes will enable significant advances both in our understanding of each subgroup of NSs as well as of the population as a whole. We present these groups separately for simplicity; however, pulsars whose radio emission properties bridge sub-populations or in other ways stand out from the rest could be the key to understanding possible evolutionary paths within the NS population. Finding new members of the existing groups of pulsars which bridge sub-populations as well as pulsars which form new bridges across sub-populations requires efficient and sensitive pulsar and single-pulse searches, as well as regular monitoring of a large number of sources and joint studies of their emission properties at radio frequencies and beyond.

The idea of a complete census of Galactic NS with the SKAO was initially presented in the first SKA Science Book (Cordes et al., 2004). A lot of the background and ideas discussed in this paper were further developed and presented in Tauris et al. (2015a) as part of the 2015 SKA Science book. Since then, the field has grown and evolved significantly. Here, we provide an update to the 2015 chapter, taking into account advances in the field, as well as changes made to the design of the SKAO telescopes in the last 10 years.

2 Magnetars and High B-field Radio Pulsars

Magnetars are NSs with extremely strong inferred surface magnetic field strengths. Their X-ray luminosity often exceeds the rotational energy budget, making their $10^{13} - 10^{15}$ G magnetic field their main energy resource (Duncan and Thompson, 1992). They are frequently discovered as X-ray transients, which erupt with bursts, outbursts, and giant flares observed in X-ray and γ -ray emission. The energy required to produce such an outburst is higher than that available from spin down alone, and magnetars are instead thought to be powered by the decay of their enormous magnetic fields (Duncan and Thompson, 1992). There are currently about 30 NSs that showed magnetar-like behaviour (see the McGill Magnetar Catalog² and Rea and De Grandis 2026), 7 of which have also been detected in the radio band. The on-set of radio emission in these sources

¹<https://www.atnf.csiro.au/research/pulsar/psrcat> (Manchester et al., 2005)

²<https://www.physics.mcgill.ca/~pulsar/magnetar/main.html> (Olausen and Kaspi, 2014)

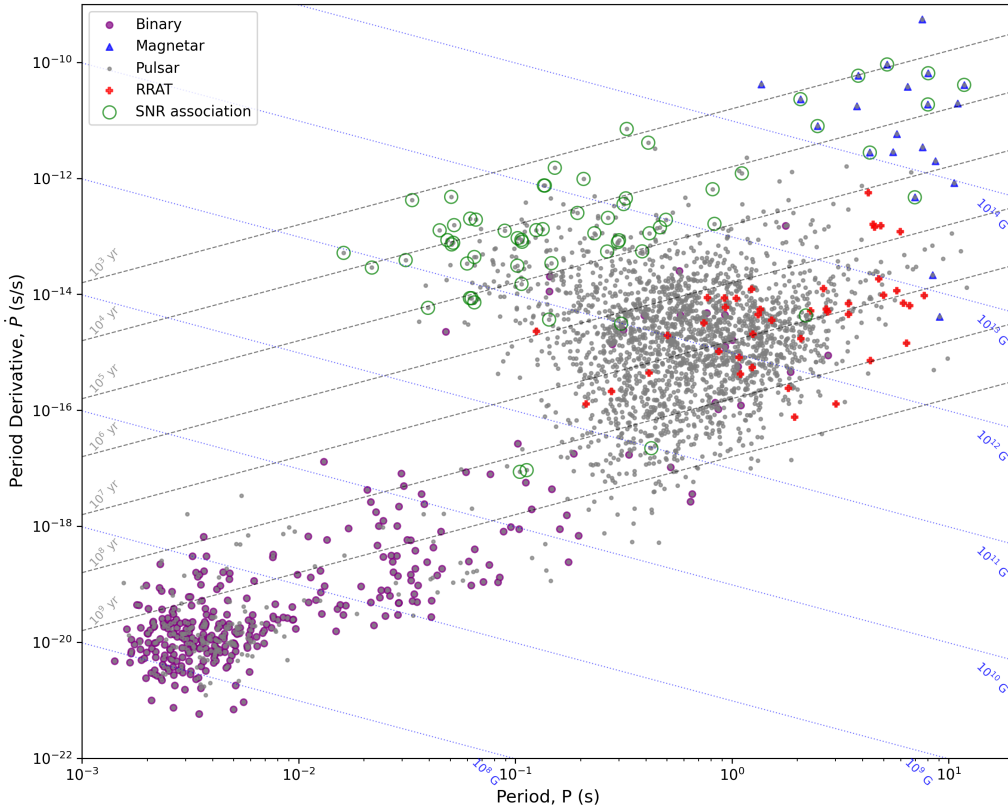


Figure 1: Distribution of 2752 pulsars in the $P - \dot{P}$ diagram. These are all the currently known pulsars that have both period and period derivative values listed. Lines of constant characteristic age and constant surface magnetic field strength are shown. Data taken from the *ATNF Pulsar Catalogue* version 2.6.1 in June 2025 (Manchester et al., 2005, <https://www.atnf.csiro.au/research/pulsar/psrcat>).

seems to be connected to their X-ray outbursts, and fade with time after the outburst. During the radio-active phase, the radio emission from magnetars is highly variable as observed as changes in the flux density, linear and circular polarisation, pulse spin down, single-pulse emission, and spectral index. The variability is highest directly after the radio emission on-set, and stabilises with time until the radio emission seems to eventually turn off in most of the cases (for recent reviews of magnetars and their emission, see Kaspi and Beloborodov, 2017; Rea and De Grandis, 2026).

The evolutionary connection between magnetars and other types of NSs is still a matter of debate. The evidence for magnetars not being a distinct class, but one sub-group of the larger pulsar family, is increasing. New sources are being discovered that exhibit magnetar-like behaviour, e.g. the Central Compact Object RCW103 (Rea et al., 2016), and high B-field radio pulsars like J1119-6127 (Archibald et al., 2016) or the Kes75 PSR J1846-0258 (Gavriil et al., 2008), which have all shown magnetar-like outbursts in X-ray emission. The high B-field pulsars are sources that mostly appear as conventional rotational powered pulsars, but which have magnetar-strength inferred surface magnetic fields. Observations using X-ray telescopes, such as Chandra and XMM-Newton, have also shown that when comparing pulsars of similar age, the higher B-field ones show higher levels of thermal X-ray emission than lower B-field pulsars (Kaspi and McLaughlin, 2005; Zhu et al.,

2011).

In the last few years, new magneto-thermal models have been developed, which aim to explain the apparent diversity of magnetars with other NS sources as an evolutionary pathway rather than a different type of object (e.g. [Viganò et al., 2013](#); [Gourgouliatos et al., 2016](#); [Dehman et al., 2023a](#); [Ascenzi et al., 2024](#); [Igoshev et al., 2025](#)). This idea is also supported by the measurement of braking indices (defined as $n \equiv P\ddot{P}/\dot{P}^2$) for a few pulsars, e.g. PSR J1734–3333 ([Espinoza et al., 2011](#)), with a braking index of $n = 0.9$ seems to be moving towards the magnetar region of the $P - \dot{P}$ diagram (see Fig. 1). More measurements of this type will help with the aim to understand the connection between different classes of pulsars. If these new magneto-thermal models are correct, they will have a large impact on the understanding of birth rates for both magnetars and for other sub-groups of NSs.

Another important area of study is the connection of magnetars with other transient events, such as Gamma Ray Bursts, superluminous supernovae, and Fast Radio Bursts (FRBs). In particular, the possibility that magnetars generate at least some FRBs has been a major advance in the last few years. FRBs are extremely bright, millisecond duration radio bursts of extra-galactic origin ([Lorimer et al., 2007](#); [Thornton et al., 2013](#)). Despite almost a thousand of these bursts having now been published, some repeating and some observed only once, the origin of FRBs is still unknown³. One very promising theory involves single pulses of radio emission from magnetars, and with the discovery of an FRB-like single-pulse burst from the Galactic magnetar SGR 1935+2154 ([Bochenek et al., 2020](#); [CHIME/FRB Collaboration et al., 2020](#); [Scholz and Chime/Frb Collaboration, 2020](#)), it is increasingly likely that magnetars are the source of at least some FRBs.

The high sensitivity of the SKAO telescopes will help address a range of questions relating to magnetars and high B-field pulsars, such as, are most magnetars truly radio quiet, and for those that have been observed in the radio band, has their radio emission really turned off in quiescence? Some studies have suggested that at least for some sources, this is really the case (e.g. [Bai et al., 2025](#)). Regular monitoring of magnetars and faint high-B pulsars for glitches, pulse profile changes, intermittency, timing variabilities, as well as more measurements of braking indices, would increase our understanding of the connection between the NS classes. New X-ray all-sky monitors (e.g. the Einstein Probe, [Yuan et al., 2022](#)) may soon identify many more high B-field pulsars via their X-ray outbursts. These sources will initially be characterised in the X-ray band by current and future X-ray telescopes, such as NewAthena ([Cruise et al., 2025](#)), and follow-up in the radio band will be crucial to form a complete picture of these sources. On the other hand, finding more high B-field pulsars with the SKAO telescopes will enable more follow-up X-ray observations, and this synergy with X-ray telescopes will add to our general understanding of NS.

3 Central Compact Objects and Neutron Stars in Supernova Remnants

Central Compact Objects (CCOs) are young isolated NSs in young ($\lesssim 10$ kyr) supernova remnants (SNRs) without known pulsar wind nebulae (e.g., [Pavlov et al. 2004](#)). There are currently 10 CCOs

³FRBs are listed in the Transient Name Server: <https://www.wis-tns.org/> and can also be found on the Blinkverse webpage: <https://blinkverse.zero2x.org/overview>

and at least 4 candidates (Ferrand and Safi-Harb, 2012)⁴, for a review, see De Luca (2017)⁵. CCOs have thermal X-ray spectra and based on these observations alone, CCOs are difficult to distinguish from quiescent magnetars. One (former) CCO in SNR RCW 103 has shown distinct magnetar-like behaviour as well as a 6.7-hr X-ray periodicity (e.g., Rea et al. 2016). Spin characteristics ($P \sim 0.1 - 0.4$ s, $\dot{P} \sim 10^{-17}$ s/s) have been measured for three CCOs (e.g., Gotthelf et al. 2013a; Halpern and Gotthelf 2010) placing them in an underpopulated part of the $P - \dot{P}$ diagram (see Figure 3) and implying surprisingly low dipole magnetic field strengths of $\sim 10^{10}$ G. For two CCOs (Gotthelf et al., 2024; Gotthelf and Halpern, 2020) the timing behaviour can be well modelled by one or more small glitches, or by extraordinary timing noise. Recently, one of these CCOs (1E 1207.4-5209) has been detected in the radio band using deep MeerKAT observations (Zhang et al., 2025). This is the only CCO with confirmed radio emission so far, despite deep searches (e.g., Turner et al. 2024; Lu et al. 2024). CCOs are among the least understood young NS populations with different models proposing buried and re-emerging magnetic fields of normal or magnetar strengths, on-going accretion from fallback disks, or births with unusually low magnetic fields; e.g., Ho (2011); Gençali and Ertan (2024); Halpern and Gotthelf (2010).

Gaensler et al. (2000) estimated the birth rate of CCOs to be at least ~ 0.5 century⁻¹, marking CCOs as a significant contributor to the so-called “NS birthrate problem” – too many NSs in comparison to the known Galactic supernova rate if one assumes all the various NS manifestations are evolutionarily independent (Keane and Kramer, 2008). Later on, Kaspi (2010) refined this value to ~ 0.0004 year⁻¹, but with the small numbers known and the uncertainties in their evolution, birth rate estimates are still highly model dependent and more work is required in this area going forward. To probe the CCO evolution and their unusual location in the $P - \dot{P}$ diagram, there have been a few unsuccessful searches for CCO descendants (so-called orphaned CCOs) (Gotthelf et al., 2013b; Luo et al., 2015). The best candidate for a CCO descendant is Calvera, a $P = 59$ ms NS with thermal X-ray emission, a supernova remnant association, and a magnetic field strength of 4.4×10^{11} G that is intermediate between CCOs and the normal pulsar population (Rigoselli et al., 2024). So far, Calvera remains undetected at radio frequencies.

The SKAO sensitivity and spatial resolution will allow understanding of CCOs and their links with the overall NS population in multiple ways: (i) The SKAO can determine whether the other known CCOs are radio emitters and, if so, measure their spin periods and rate of spin-down. Sampling different CCO ages (as determined from the SNR ages) could then help probe the time of the onset of radio emission, in the cases where it was detected. For such studies more CCOs are required since the current CCO age span, 0.3 – 10 kyr, hinges on individual objects. (ii) The SKAO can search for radio-emitting pulsars in SNRs, some of which may turn out to be CCOs. Timing of the newly discovered radio pulsars will help to constrain the birth period distribution of NSs. There are $\gtrsim 300$ known SNRs and $\gtrsim 200$ SNR candidates (e.g. Anderson et al., 2017; Hurley-Walker et al., 2019; Dokara et al., 2021; Green, 2022), a sample that keeps growing with the search of radio images using more sensitive radio telescopes. Recent deep MeerKAT searches (down to flux limits of ~ 30 μ Jy) of SNRs and CCOs illustrate the feasibility and potential of such deep radio surveys of SNRs (e.g., Turner et al. 2024). The detection of radio pulsations in CCO 1E 1207.4-5209 shows that at least

⁴<http://snrcat.physics.umanitoba.ca/SNRtable.php>

⁵<http://www.iasf-milano.inaf.it/deluca/cco/main.htm>

some CCOs are radio emitters (Zhang et al., 2025). The radio emission from this source is weak ($33 \mu\text{J}$ at 816 MHz), suggesting that other CCOs may also be detectable with a more sensitive radio telescope. Using a setup similar to that in Zhang et al. (2025) with the full AA*/AA4 SKA-Mid⁶, would give an improvement of a factor of 2.4 (AA*) to 3 (AA4) of their $\sim 10 \mu\text{J}$ sensitivity limit. (iii) The SKAO can also search for CCO descendants. This could be achieved through deep radio searches of enigmatic objects such as Calvera. A periodic and single pulse survey with the SKAO telescopes will also probe the underpopulated CCO location in the $P - \dot{P}$ diagram as well as the adjacent regions where CCO descendants may stage their radio appearance. (iv) The SKAO will be crucial in identifying and characterising new NS candidates found at other wavelengths such as X-rays. This could be done by e.g. following up the large number of X-ray sources discovered by eROSITA (see Merloni et al., 2024). Multiwavelength synergy effects will be particularly important for CCOs considering the aforementioned possible links of CCOs with magnetars and the propensity to high-energy outbursts of the latter.

4 Rotating Radio Transients and Intermittent Pulsars

Since their discovery by McLaughlin et al. (2006) using single-pulse search techniques, rotating radio transients (RRATs) represent a complementary means of discovering and studying the spin-powered population of NSs. Care should be exercised since the simplest observational definition of an RRAT is sensitivity-dependent: for a given radio telescope, an RRAT is a pulsar that is more easily detectable through a single-pulse search compared to traditional techniques designed to reveal periodic sources (most commonly Fast Fourier Transforms or Fast Folding Algorithms). It is possible to quantify this for both nulling and non-nulling pulsar cases (as given in Eqns. 1 and 2 of Burke-Spolaor, 2013). A comparison of RRAT pulses versus other types of NSs is given in Fig. 2.

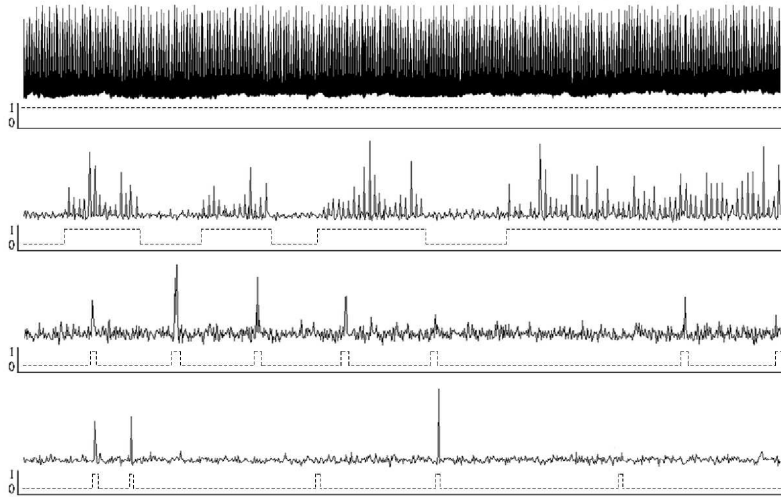


Figure 2: Time series (all of equal duration) taken from Burke-Spolaor (2013) showing radio emission from a variety of sources (top to bottom: the Vela pulsar, PSR J1646–6831 (a nulling pulsar), RRAT J1647–36 and RRAT J1226–32). The binary scales show an estimated representation of the null/emission state.

⁶see section 11 for a description of the SKAO Array Assemblies

In the twenty years that have elapsed since the discovery of the RRATs, single-pulse search algorithms are now an integral part of pulsar surveys. To date, while 211 RRATs are currently known⁷, due to the difficulties in detecting them, not all of the parameters are well measured. In a recent statistical analysis, [Abhishek et al. \(2022\)](#) found that, for the 42 RRATs with measured period derivatives (\dot{P}), these sources are preferentially found toward the upper right of the $B - P$ diagram, with an average characteristic magnetic field strength of 6.3×10^{12} Gauss (see also [Cui et al., 2017](#)). A recent population analysis by [Agarwal et al. \(2026\)](#) attempted to constrain the underlying parameters of the population, which has many similarities with that of radio pulsars, although there is evidence for a larger scale height for RRATs: 600 ± 200 pc, almost double that of the canonical pulsar population (see, e.g., [Faucher-Giguère and Kaspi, 2006](#)).

The higher than average B and P values for the RRATs compared to the normal pulsar population is significant. The longest period reported for an RRAT so far is 11.9 s ([Zhou et al., 2023](#)), although there are known candidates with even larger periods (see below). An outstanding question is the connection between RRATs and other long-period pulsars, and the emerging population of long-period transients (see Section 10). In addition, despite the small sample size currently observed, the Galactic population of RRATs is expected to be similar to that of normal pulsars (see, e.g., [McLaughlin et al., 2006](#); [Agarwal et al., 2026](#)). A larger sample size as a result of SKAO surveys will not only constrain the populations, but also provide individual objects to study at other wavelengths. Currently, only RRAT J1819–1458 has detectable X-ray emission ([McLaughlin et al., 2007](#)). The superior sensitivity of the SKAO, and other emerging instruments, is expected to play a role in a number of important, and currently poorly understood, aspects of the RRAT population. Firstly, in concert with the increasing sample sizes of other NS populations, enhanced statistics of the currently known RRATs, and the many that are expected to be discovered, should be able to shed light on the connection between pulsars, RRATs and long-period pulsars. A recent MeerKAT survey by [Turner et al. \(2025\)](#) discovered an additional 26 RRATs and RRAT candidates, including RRAT candidate PSR J2218+2902 which has a spin period of 17.5 s. For currently known RRATs, to improve constraints on the emission process(es), high-sensitivity observations are urgently required to probe the presence of emission during epochs where no pulses are currently detectable. We note that a combination of the precise localisation of the RRAT sources through real-time detection and imaging of single pulses and the commensal observing modes of the SKAO telescopes will greatly facilitate the measurement of the crucial \dot{P} values, as demonstrated for SKAO precursors such as MeerKAT ([Turner et al., 2025](#)). A more complete census of the RRAT population could also elucidate the spectral properties of RRATs, provide braking indices through long-term timing, and the precise localisations will allow for rapid follow up at non-radio wavelengths.

In addition to RRATs, a very important phenomenon in the pulsar population is that of pulsar intermittency. This behaviour, in which the pulsar switches between an ON and OFF state accompanied by an increase in spin-down rate during the ON-state, was first seen in PSR B1931+24 by [Kramer et al. \(2006\)](#) and has subsequently been observed in only a handful of other pulsars ([Lorimer et al., 2012](#); [Camilo et al., 2012](#); [Lyne et al., 2017](#)). A larger number of pulsars show switching between the ON and OFF states at shorter time scales, from seconds to hours, and are generally called nulling

⁷An up-to-date list of RRATs can be found within the ATNF pulsar catalogue.

pulsars. These state changes are too short to allow us to see any potentially associated changes in the spin-down rate. Some pulsars also show switching between different modes of emission, which manifest as differences in pulse profiles or flux density. Such sources are called mode-changing pulsars, and some of the ones with the longest mode-changing timescales have also shown different spin-down rates for different modes (e.g. Lyne et al., 2010). Since these different groups of sources have such similar properties, it is easy to suspect that the emission changes have the same underlying origin. Many models have been developed to explain the phenomena; some consider the plasma in the magnetosphere and how it is connected to the global charge distribution (e.g. Timokhin, 2010; Kalapotharakos et al., 2012; Li et al., 2012; Melrose and Yuen, 2014), others suggest variations in the particle acceleration region (Szary et al., 2015) or a twisted magnetosphere (Huang et al., 2016).

Intermittent, mode-changing, and to some extent nulling pulsars, provide excellent opportunities to study how a pulsar’s spin-down is related to its radio emission. It is therefore very important to find more of these types of sources. The SKAO telescopes, with their excellent sensitivity and wide field of view, will be significant in this search. In addition, high-sensitivity observations with the SKAO telescopes will be able put better limits on the radio emission in the OFF-state, and by using the multibeaming capabilities of the pulsar timing backend, higher cadence observations will help in determining more exact switch times between states in known intermittent pulsars.

5 Isolated Pulsar Evolution on the P - \dot{P} Diagram

Observing pulsars provides a snapshot of a fraction of the pulsar population at present. As NSs have formed throughout the Galaxy’s history, any such snapshot provides information about NSs across a range of ages. Studying present-day properties for a sufficiently large number of stars, thus allows us to constrain population-level properties. The increase in the known population as resulting from planned pulsar surveys with the SKAO telescopes will hence play a crucial role in our understanding of the population as a whole. In this section, we will summarise the current state of evolutionary NS population modelling and present predictions for the isolated pulsar population observable with the SKAO in the AA* and AA4 configurations.

A key diagnostic for analysing pulsar populations is the period-period derivative (P - \dot{P}) diagram. This is particularly crucial when focusing on isolated pulsars, as the P - \dot{P} diagram enables the identification of distinct NS classes and possible evolutionary relationships. Mapping between the observed population (currently a few thousand isolated sources predominantly seen in the radio) and the underlying population also requires the incorporation of observational biases and limitations (Keane et al., 2025). Once incorporated, these population synthesis approaches allow us to extract information on NS birth properties, birth rates, and the fundamental laws that govern their evolution (Lorimer, 2004; Faucher-Giguère and Kaspi, 2006; Bates et al., 2014; Johnston and Karastergiou, 2017). Recent advances in this area have involved the implementation of updated theoretical models, the increase of available computational resources, and adaption of machine learning techniques.

For isolated NSs, birth parameters shaping the P - \dot{P} distribution fall into two categories: dynamical properties and magneto-rotational characteristics. The birth locations of pulsars are relatively

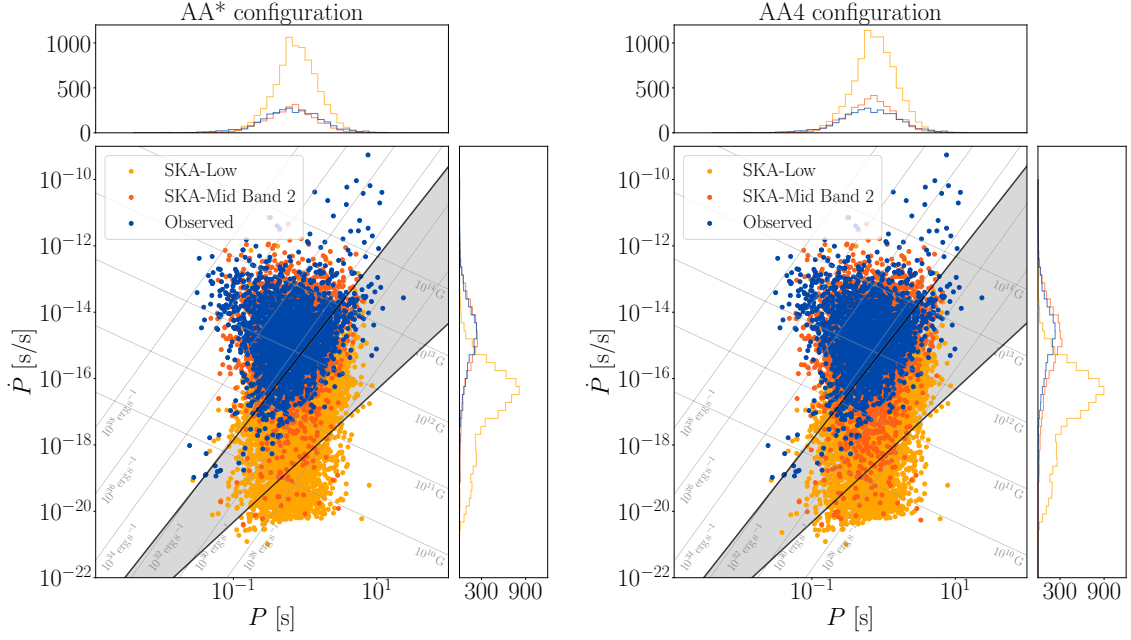


Figure 3: P - \dot{P} diagrams for the expected population of isolated pulsars observed with SKAO in the AA* (left) and AA4 (right) configurations corresponding to Survey Option 3 for the evolutionary population synthesis approach outlined in Keane et al. (2025). The total numbers of sources predicted in this simulation are about 8100 for SKA-Low and 2600 for SKA-Mid in the AA* configuration, and 8800 for SKA-Low and 3400 for SKA-Mid in the AA4 configuration. We show the currently observed population in blue (~ 2300 sources excluding millisecond pulsars, data taken from the ATNF Pulsar Catalogue v2.5.1; Manchester et al. (2005), <https://www.atnf.csiro.au/research/pulsar/psrcat/>), and pulsars detected with SKAO Low and Mid Band 2 in yellow and orange, respectively. Lines of constant rotational energy loss and dipole magnetic field strength are shown in grey. The black lines show extreme versions of the pulsar death lines below which radio emission has been proposed to cease and delimit the so-called “death valley” shaded in grey (Chen and Ruderman, 1993). Note that these population synthesis simulations take into account the natural fading of the radio emission but do not account for sudden emission switch-off or occasional switch-on of stronger emission that may be detectable with single-pulse searches (for a recent example, see Rajwade et al. 2025).

well understood (Yusifov and Küçük, 2004), but uncertainties remain regarding the kick velocity distribution imparted during the supernovae (see Section 9 below). This will primarily affect future all-sky surveys which will detect older pulsars far from the Galactic plane. Magneto-rotational properties, in turn, depend on natal magnetic field strengths, B , and initial rotation periods. The former are typically assumed to follow a log-normal distribution (Faucher-Giguère and Kaspi, 2006; Popov et al., 2010; Gullón et al., 2014, 2015; Cieřlar et al., 2020; Igoshev et al., 2022), with recent studies inferring $\mu_{\log B} \sim 13.1$ and $\sigma_{\log B} \sim 0.5$ (Graber et al., 2024; Pardo-Araujo et al., 2025) based on updated magnetic-field evolution models (see below). The functional form of the period distribution, initially assumed to be Gaussian (Faucher-Giguère and Kaspi, 2006; Cieřlar et al., 2020), is more difficult to constrain. This is due to the coupled evolution of spin period, magnetic field strength and misalignment angle and the fact that NSs lose memory of their initial spin periods after a characteristic evolutionary time-scale (see Graber et al., 2024, for details). Based on simplifying assumptions of the pulsar spin-down, two recent analyses of around 70 young

pulsars in supernova remnants found evidence for a log-normal (Igoshev et al., 2022) and a Weibull distribution (Du et al., 2024), with differences arising from the treatment of observational selection effects. Based on the log-normal P distribution, two neural network-based studies have inferred $\mu_{\log P} \sim -1$ to -0.7 and $\sigma_{\log P} \sim 0.4$ to 0.6 (Graber et al., 2024; Pardo-Araujo et al., 2025).

While dynamical properties are easily evolved via the solution of Newtonian equations of motion in the Galactic potential, different approaches have been used to evolve magneto-rotational properties. Many earlier works assume the NS spin-down to be dipolar, neglect misalignment angle variations, and do not account for the possibility of magnetic field decay. While such assumptions enable fast generation of synthetic pulsar populations, they neglect key physics of realistic NSs. In particular, simulations of plasma-filled magnetospheres (Spitkovsky, 2006; Philippov et al., 2014) indicate that the spin-down is governed by two coupled differential equations, combining spin-down contributions from the magnetic dipole and the plasma currents,

$$\dot{P}(t) = \frac{\pi^2 B(t)^2 R^6}{c^3 IP(t)} [1 + \sin^2 \chi(t)] \quad \text{and} \quad \dot{\chi}(t) = -\frac{\pi^2 B(t)^2 R^6}{c^3 IP(t)^2} \sin \chi(t) \cos \chi(t), \quad (1)$$

where the misalignment angle χ is distributed uniformly at birth. Here, c denotes the speed of light, and R and I the NS radius and moment of inertia, respectively. Assuming these equations are correct, they imply that χ decreases as pulsars slow down (for other models, see Novoselov et al. 2020; Toropov et al. 2024). The exact behaviour of such evolutionary models, however, also requires a prescription for magnetic field evolution, $B(t)$, commonly assumed to be exponential or power-law like (Aguilera et al., 2008), based on Ohmic dissipation and the Hall effect, respectively. While these provide general insights into field changes, multi-dimensional simulations are ultimately needed to accurately capture field evolution in NSs (De Grandis et al., 2020; Viganò et al., 2013, 2021; Dehman et al., 2023b; Ascenzi et al., 2024). Several recent studies incorporate two-dimensional magneto-thermal simulations into pulsar population synthesis, finding field decay crucial to match observations (e.g., Cieřlar et al., 2020; Gullón et al., 2014; Dirson et al., 2022; Graber et al., 2024; Shi and Ng, 2024). While early-time field evolution is less important for radio pulsars, it is essential for modelling young magnetars as suggested by Gullón et al. (2015); Sautron et al. (2025). Including magnetars and radio-quiet NSs in future population synthesis pipelines will thus help improve natal field constraints for strongly magnetised sources, poorly constrained by radio observations alone.

Accounting for misalignment angle and magnetic field evolution, pulsars are expected to migrate from the top-left to the bottom-right in the P - \dot{P} plane as they age. As they do so, the stars' available spin-down power decreases. In addition, narrower pulses are measured with increasing pulse periods for most pulsars (Posselt et al., 2021). This can be interpreted as shrinking emission beams. Consequently, several modern population synthesis approaches can reproduce the observed radio pulsar population without invoking a “death line” where radio emission ceases (Gullón et al., 2015; Graber et al., 2024; Pardo-Araujo et al., 2025; Shi and Ng, 2024). However, the fading of old NSs and their P - \dot{P} locations also depend on radio emission models. The radio luminosity, L , is typically assumed to be proportional to the spin-down power, $L \propto |\dot{E}_{\text{rot}}|^\alpha \propto P^{-3\alpha} \dot{P}^\alpha$ or more generally $\propto P^\beta \dot{P}^\gamma$. For example, Cieřlar et al. (2020) found $\beta \sim -0.37$ and $\gamma \sim 0.26$, while Pardo-Araujo et al. (2025) inferred $\alpha \sim 0.7$ (see also Shi and Ng, 2024) and Posselt et al. (2023) obtained $\alpha \sim 0.15$. These estimates are, however, not directly comparable, as Cieřlar et al. (2020) model the pseudo-

luminosity and introduce a period-dependent beaming factor which is set as a constant by [Posselt et al. \(2023\)](#), while [Pardo-Araujo et al. \(2025\)](#) considers the intrinsic luminosity, a time-dependent beaming model and pulse propagation through the interstellar medium. Figure 3 summarises our current understanding of isolated pulsar evolution and makes predictions for SKAO observations with the AA* and AA4 baselines (see Section 11). We highlight that the SKAO telescopes will detect many faint, old pulsars in the lower-right region of the $P-\dot{P}$ plane, enabling us to refine highly uncertain emission models and death-line physics ([Oswald et al., 2025](#)). This is especially relevant for the newly discovered class of long-period radio emitters (see Section 10). Consistent radio flux measurements alongside period and period derivative data will be crucial to understanding their emission ([Cieřlar et al., 2020](#); [Pardo-Araujo et al., 2025](#); [Keane et al., 2026](#)). Moreover, these low \dot{P} sources will also be interesting for continuous gravitational wave searches and exploring the ‘spin-down limits’ of the corresponding gravitational wave strain ([Abac et al., 2025b](#)).

While population synthesis broadly captures the observed radio pulsar population, not all pulsars move downward in the $P-\dot{P}$ plane. Measuring braking indices, reveals deviations from the dipolar spin-down expectation of $n = 3$. While some of these are readily explained by field decay, several young pulsars show $n \simeq 2$ ([Espinoza et al., 2017](#)) or well below (e.g. [Espinoza et al., 2011](#)), indicating upward motion in the diagram. This may be linked to magnetic field growth ([Ho, 2015](#)) but is complicated by pulsar glitches affecting long-term spin evolution ([Lower et al., 2021](#)) and general long-term variability ([Lower et al., 2025](#)). Although such young sources may provide insights into internal field evolution and dense matter physics ([Basu et al., 2026](#)), their impact on future pulsar population studies is likely minimal, as the SKAO telescopes will predominantly probe older sources that are less prone to exhibit glitches. However, such effects may be relevant when modelling central compact objects, magnetars, and high-B field pulsars (see Sections 2–3). In general, monitoring of time-variable braking indices for the bulk of the pulsar population may shed light on the evolution of these sources within the $P-\dot{P}$ plane and the validity of modelling assumptions such as inferred magnetic field strengths and characteristic ages.

As isolated pulsar modelling grows in complexity, robust inferences become more challenging. Traditional statistical techniques such as Kolmogorov-Smirnov tests, χ^2 analyses, and Markov Chain Monte Carlo (MCMC) methods struggle with high-dimensional parameter spaces and complex simulation frameworks. Recent studies ([Graber et al., 2024](#); [Pardo-Araujo et al., 2025](#); [Sautron et al., 2025](#)), highlight the promise of simulation-based inference with neural networks for overcoming these challenges. In the future, machine-learning approaches may also finally enable robust comparisons between physical models, which has not been possible to date. An SKAO telescope pulsar census (see Section 11 and [Keane et al. 2026](#) for details) will be instrumental in advancing these studies by providing comprehensive, consistent pulsar measurements, particularly when combined with all-sky surveys in other wavebands.

6 Pulsar Recycling and Formation of Exotic Binaries and Triples

The widely accepted formation channel for fast-spinning millisecond pulsars (MSPs) is the recycling scenario ([Alpar et al., 1982](#); [Radhakrishnan and Srinivasan, 1982](#); [Bhattacharya and van den Heuvel, 1991](#)), in which a NS is spun up through mass and angular momentum accretion from a companion

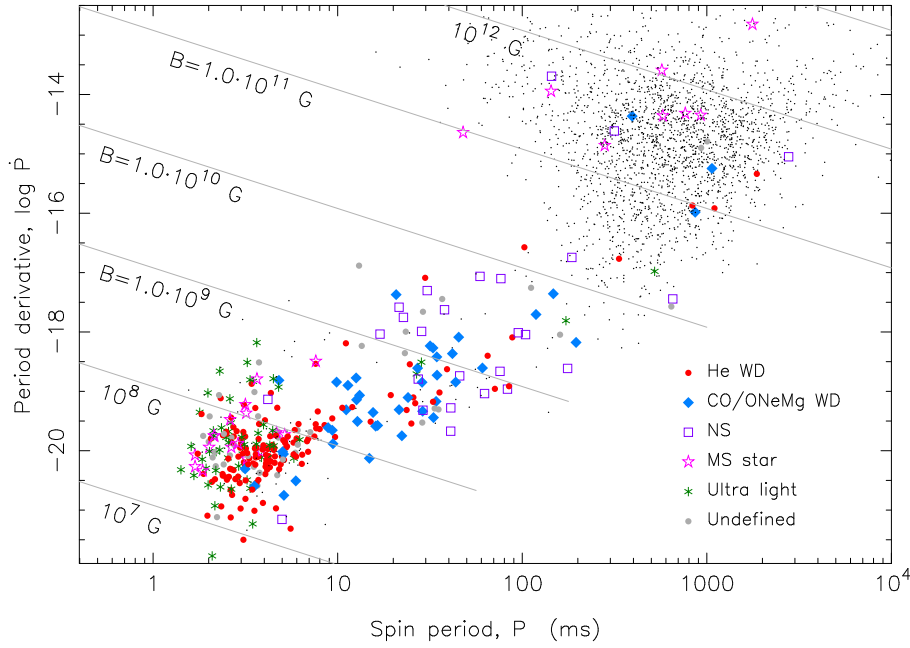


Figure 4: Distribution of 346 binary radio pulsars in the PP -diagram. The nature of the companion stars is indicated with different symbols. Isolated pulsars are represented with a dot. Lines of constant surface B-field flux density are shown. Data taken from the *ATNF Pulsar Catalogue* version 2.6.0 in February 2025 (Manchester et al., 2005, <https://www.atnf.csiro.au/research/pulsar/psrcat>).

star. The outcome depends on the initial binary configuration and subsequent evolutionary phases (see Tauris and van den Heuvel, 2023, for a detailed review), leading to recycled pulsars with spin periods ranging from just a few milliseconds (‘fully recycled’) to several tens or hundreds of milliseconds (‘mildly recycled’). These NSs can orbit a diverse set of companion stars (see Figure 4) — ranging from compact objects (white dwarfs, NSs, or black holes) to main-sequence stars, or even ultra-light planetary-mass bodies. Observationally, of the 638 recycled pulsars discovered with $P < 30$ ms (Manchester et al., 2005) — 426 in the Galactic disk and 212 in globular clusters (GCs) — nearly 60% are found in binary systems, most commonly with helium white dwarf (He-WD) companions in circular orbits. For comparison, the binary fraction among young radio pulsars is estimated to be at most 5–8% (Antoniadis, 2021).

A small but growing number of MSPs with unusual properties have been discovered, including the ‘triple pulsar’ PSR J0337+1715, which is orbited by two WDs (Ransom et al., 2014; Voisin et al., 2025); PSR J1903+0327, which has a $\sim 1 M_{\odot}$ main-sequence companion in a long-period, eccentric orbit (Freire et al., 2011); the now established class of enigmatic eccentric MSPs (eMSPs), potentially indicating a hierarchical triple system origin (Champion et al., 2008; Deneva et al., 2013; Antoniadis et al., 2016; Barr et al., 2017; Serylak et al., 2022; Grunthal et al., 2024). Another intriguing case is the MeerKAT discovery of PSR J0514–4002E (Barr, Dutta, et al. 2024), which orbits either a low-mass BH or a very massive NS — likely the remnant of a former merger event in the dense environment of its host GC.

Thanks in large part to the launch of the Fermi γ -ray Space Telescope — which has provided valuable

targets for deep follow-up pulsar searches in the radio band (Abdo et al., 2009) — an ever-growing number of MSPs has been discovered in binaries with light, semi-degenerate companions. These pulsars are often characterised by eclipses of their pulsed radio signal over large portions of the orbit, caused by matter surrounding the system. This material is either ablated from the companion star by the pulsar wind or may represent residual mass still being ejected from the companion’s Roche lobe. These so-called spiders (Roberts, 2013) are classified into two subgroups: *black widows*, with companion masses typically well below $0.1; M_{\odot}$, and *redbacks*, with companion masses of $\sim 0.1\text{--}0.3; M_{\odot}$ (marked as "MS star" in Fig. 4). It remains debated whether these are two distinct populations (Chen et al., 2013), or instead represent an evolutionary sequence (Benvenuto et al., 2014; Misra et al., 2025).

A compelling evolutionary link between accretion-powered and rotation-powered binary pulsars is provided by the discovery of ‘transitional MSPs’ (tMSPs), which alternate between accretion-powered high-energy pulsed emission and rotation-powered radio pulsations (Archibald et al., 2009; Papitto et al., 2013). The radio pulsars in tMSPs appear as redback systems, and offer the most direct and compelling observational evidence in support of the recycling scenario. While there is now ample evidence that this scenario is broadly correct, many details remain poorly understood. Some of the open questions (e.g. Tauris et al., 2012, and references therein) include: mechanisms behind accretion-induced decay of the surface magnetic field (but see also Cruces et al., 2019); the maximum attainable spin rate of an MSP; the Roche-lobe decoupling phase; the nature and physics of accretion torque reversals; the spin-up line.

The SKA-Mid telescope will be particularly well suited for detecting ultra-compact binary pulsars in the final stages of their recycling — potentially revealing the long-sought sub-ms pulsar (see Figure 5). The MSP currently known to have the fastest spin rate PSR J1748–2446ad, has a period of 1.4 ms (Hessels et al., 2006). Its location in a globular cluster and its extreme spin raise the question of whether multiple recycling episodes in a dense stellar environment (Verbunt and Freire, 2014) might be a necessary condition for producing a sub-ms pulsar. High time and frequency resolution, combined with high instantaneous sensitivity, are the most important factors to enable finding the shortest pulse periods (e.g. Ransom et al., 2005; Hessels et al., 2006). With the SKAO, in the ‘Detected Filterbank’ observing mode, data can be sampled as fast as every 100 ns and use the full width of the observing band⁸ for a small number of beams (up to 16). This high possible time resolution coupled with high telescope sensitivity will enable astronomers to probe the period distribution down to sub-millisecond periods in targeted searches. See Bagchi et al. (2026) for an extended discussion on searching for short period pulsars in Globular Clusters.

Over the past decade, the number of known recycled pulsars has nearly doubled. In addition to the increase enabled by targeted observations of Fermi sources, as described above, a key driver of this growth has been the improved sensitivity of radio instrumentation. Historic telescopes — such as the Murriyang telescope at Parkes in Australia and the Effelsberg telescope in Bonn, Germany — have been upgraded with ultra-wideband receivers, while new, highly sensitive facilities like the FAST telescope in China and the MeerKAT array in South Africa have significantly increased the

⁸See <https://www.skao.int/en/science-users/646/year-life-ska> (date: 2025-06-13) for details on SKAO observing modes.

discovery rate, enabling the detection and detailed study of increasingly peculiar systems.

Improvements in instrumentation often lead to significantly higher data rates, driven by larger bandwidths combined with higher time and frequency resolution. As a result, the development of reliable and efficient software for processing the growing volumes of pulsar data has been a crucial factor in the continued success of pulsar science — especially for the discovery of MSPs in compact binaries, which requires searching over a vast parameter space. Key advances include acceleration and jerk search techniques, GPU-accelerated pipelines such as PRESTO (Ransom, 2011), and template banking algorithms (e.g. Peasoup, Barr, 2020).

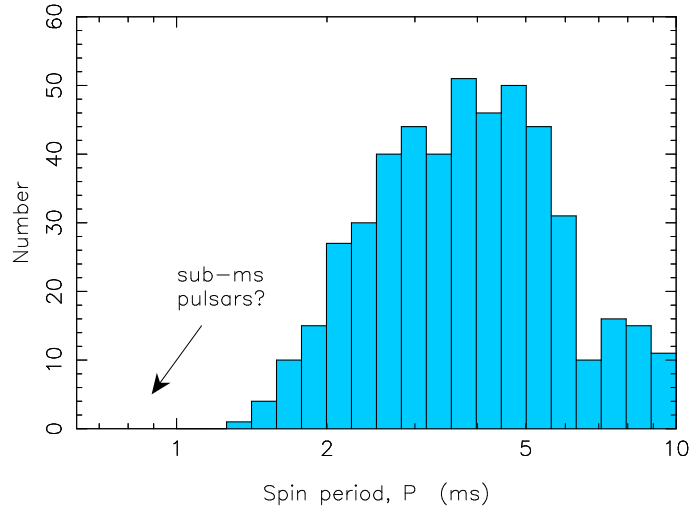


Figure 5: Distribution of spins of 485 radio MSPs with $P < 10$ ms. After Tauris and van den Heuvel (2023).

7 Double Neutron Star and Neutron Star-Black Hole Systems

Double neutron star (DNS) systems represent the rare and extreme endpoint of an evolutionary journey involving two massive stars and their binary interactions. Currently, more than two dozen DNS systems are known (including unconfirmed candidates), but only in one — *the double pulsar* J0737–3037 (Burgay et al., 2003; Lyne et al., 2004) — has radio pulses been observed from both NSs. Many additional DNS systems are expected to be discovered with the SKAO telescopes in upcoming pulsar surveys (Keane et al., 2015, 2025). In combination with the LIGO–Virgo–KAGRA detections of DNS mergers, beginning with GW170817 (Abbott et al., 2017) and GW190425 (Abbott et al., 2020a), the coming decade offers a unique opportunity to refine our understanding of the formation and evolution of DNS systems (Tauris et al., 2017). This includes their accretion history during the high-mass X-ray binary stage, the common-envelope and spiral-in phase, and the subsequent so called Case BB mass transfer phase (see e.g. Delgado and Thomas, 1981), in which the first-born NS is mildly recycled while stripping the envelope of its He-star companion prior to core collapse and SN explosion (Tauris et al., 2015b).

Measurements of DNS masses, spins, orbital characteristics, and velocities provide crucial insights into their formation history and the nature of NS kicks, and are also essential for testing fundamental theories of gravity (Kramer et al., 2021). The MeerKAT discovery of PSRJ0514–4002E (Barr,

Dutta, et al. 2024), orbiting either a low-mass BH or a massive NS, represents the closest realisation to date of detecting an MSP in orbit around a BH. This source is located in the GC NGC 1851, supporting a formation scenario involving an exchange encounter. Despite population synthesis predictions (e.g. Chattopadhyay et al., 2021), such MSP+BH systems are not expected to form frequently in the Galactic field due to the short nuclear timescale of the BH progenitor, which limits the duration and efficiency of the X-ray recycling phase. Therefore, continued targeted searches in GCs or in the Galactic Centre, where similarly large stellar densities can be found, appear to offer the best chance of detecting a compact MSP+BH binary (e.g. Liu et al., 2014; Bagchi et al., 2026; Abbate et al., 2026) – unless such a system is ejected into the field, which remains a possibility.

Over the past decade, gravitational wave (GW) observations have finally revealed mergers involving extragalactic DNS and NS+BH systems, and have unequivocally linked them to short γ -ray bursts (Savchenko et al., 2017; Ajello et al., 2018). The observed properties of these merger events, together with their likely connections to Galactic DNS systems, highlight the need to better constrain the properties and formation rates of Galactic DNS and NS+BH binaries. Improved understanding of these populations will refine theoretical predictions of GW merger rates (e.g. Belczynski et al., 2008; Kruckow et al., 2018), enabling more robust comparisons with observations and providing critical feedback on population synthesis models. In addition, the past decade has brought significant advances in strong-field tests of gravity using DNS systems (Kramer et al., 2021). On the theoretical side, the first detailed simulations of close binary stellar evolution up to the onset of core collapse — leading to the second, ultra-stripped SN and the final formation step of a DNS system — have been carried out using MESA (Jiang et al., 2021).

A critical challenge in discovering pulsars in tight, eccentric binaries (such as the DNS, MSP+BH, and NS+BH systems) is their detectability: such binaries are difficult to find without enhanced acceleration or acceleration–jerk searches (e.g. Bagchi et al., 2013; Andersen and Ransom, 2018), or alternative methods such as template bank algorithms that account for all five Keplerian parameters (Balakrishnan et al., 2022). Additional complications may arise from relativistic spin-orbit coupling (e.g. Stairs et al., 2004) or perhaps even light-deflection (Doroshenko and Kopeikin, 1995; Rafikov and Lai, 2006; Hu et al., 2022; Debnath et al., 2023), which can alter the pulse profile across the orbit, thereby complicating the data analysis. However, the enhanced sensitivity of the SKAO telescopes, combined with the planned pulsar acceleration searches, will allow for high signal-to-noise pulse profiles, helping to overcome these obstacles.

8 Neutron Star Masses

High-precision radio pulsar timing is currently the most effective technique for measuring NS masses. By tracking every rotation of a pulsar over months to decades, timing models allow us to extract orbital information and, in few favourable binary systems, relativistic post-Keplerian parameters that are directly sensitive to the masses of the system’s components (Damour and Taylor, 1992). In particular, measurements of the Shapiro delay have now enabled mass estimates with uncertainties well below 15% (see Figure 3 in Basu et al. 2025).

Over the past 15 years, these timing observations have significantly expanded the NS mass distribution, confirming the existence of both high-mass and low-mass NSs. The most massive NS

discovered through pulsar timing to date is PSR J0740+6620 with a mass of $2.08 \pm 0.07 M_{\odot}$ (Fonseca et al., 2021). Discoveries like this have set critical benchmarks on the maximum attainable NS mass, specifically ruling out those nuclear-matter equations of state that are particularly soft. Additional mass constraints have come from multi-wavelength observations in spider pulsar systems, as discussed above, which suggest even heavier NSs may exist (Linares, 2019). Currently, the heaviest spider pulsar is PSR J0952–0607 with a mass of $2.35 \pm 0.17 M_{\odot}$ (Romani et al., 2022). However, to measure the mass of a spider pulsar, spectroscopy of the companion star is used to determine its radial velocity, which in turn can provide an inclination-dependent mass measurement. Estimates of the system’s inclination can then be inferred from the optical light curve, but the resulting masses are often overestimated due to uncertainties in the modelling of the heat distribution on the surfaces of the NS companions (Voisin et al., 2020b; Clark et al., 2023).

At the low-mass end, systems like PSR J0453+1559, the lightest NS candidate detected with pulsar timing with $1.174 \pm 0.004 M_{\odot}$ (Martinez et al., 2015), challenge our understanding of stellar core collapse and binary evolution (Tauris and Janka, 2019; Müller et al., 2025) suggesting possible diversity in NS formation channels. Neutron star minimum masses below $1 M_{\odot}$ as recently suggested by spectral modelling of the central compact object in a supernova remnant HESS J1731–347 (Doroshenko et al., 2022) would question our understanding of NS formation even further. However, these mass measurements are based on numerous assumptions and larger masses can explain the data equally well (Alford and Halpern, 2023). Future radio timing observations with the SKAO will be crucial to narrow down the full NS mass distributions.

Mass measurements have also been achieved by analysing gravitational waves from binary NS mergers. As the signal depends directly on the chirp mass, dependent in turn on the two component masses, a corresponding measurement together with assumptions on the NSs’ spin, allows constraints on the two NS masses. For GW170817, corresponding mass estimates are in line with those obtained from radio pulsar timing, albeit less certain (Abbott et al., 2017). In the low-mass regime, searches for sub-solar mass gravitational wave merger events have resulted in candidates, however yet no firm detection (e.g. LVK Collaboration et al., 2023). Gravitational wave observations have also opened up the study of objects in the so-called lower “mass gap” between $2 - 3 M_{\odot}$ (e.g., the secondary object in GW190814; Abbott et al. 2020b), where it is unclear whether the compact object is a NS or a black hole. Note that a similar mass-gap object, the companion of PSR J0514–4002, has now also been detected via radio timing (Barr et al., 2024), highlighting that detections in similar mass ranges can also be expected in the SKAO era. Objects with these masses directly probe the maximum NS mass and corresponding formation scenarios of compact objects.

Beyond understanding the nuclear equation of state (Basu et al., 2025), massive NS binaries also serve as laboratories for gravity (Freire and Wex, 2024; Venkatraman Krishnan et al., 2025). Timing experiments in relativistic binaries have provided stringent tests of general relativity and alternatives, especially when multiple post-Keplerian parameters can be measured. The famous double pulsar system (Kramer et al., 2021), along with pulsar–white dwarf binaries and triple systems (Voisin et al., 2020a), has yielded some of the most precise tests of gravitational theories to date. Looking ahead, the SKAO is expected to revolutionise this field. With its unprecedented sensitivity and wide-field capabilities, SKAO will perform deep, all-sky pulsar surveys that are expected to greatly

increase the number of known pulsar binaries (Keane et al., 2025). This will drastically expand the sample size of precisely timed pulsars, improving statistical analyses of the NS mass distribution and offering new opportunities for detecting extreme systems—either with exceptionally high or low masses. The discovery of new relativistic binaries through these surveys will thus enable new tests of general relativity and provide valuable data on the demographics of NS populations across different formation channels. Finally, the participation of SKAO in sensitive VLBI observations can provide the precise parallax measurements needed to calibrate distance-dependent contributions to timing observables used to test post-Newtonian gravitational theories (e.g., Kramer et al., 2021).

Moreover, synergies with other observatories will further enhance equation of state constraints. X-ray observations like those performed with NICER already provide complementary radius estimates via pulse profile modelling (Salmi et al., 2024) (especially powerful when combined with tight mass priors from pulsar timing), while gravitational wave detections from compact binary mergers contribute additional mass information. While the latter are currently uncertain, next-generation facilities will allow us to better probe the NS masses in the gravitational wave band (Abac et al., 2025a). Together, these approaches will eventually allow us to map out the full NS mass spectrum, refine the maximum and minimum NS mass, and deepen our understanding of their interiors and their role in testing gravity under extreme conditions.

9 Neutron Star Kicks and Velocities

A few years after the discovery of radio pulsars, Gunn and Ostriker (1970) noted that the vertical distribution of radio pulsars around the Galactic plane is much broader than that of their OB star progenitors, which are confined to within a few hundred pc of the plane. To explain this discrepancy, they introduced the concept of a ‘velocity kick’ — a momentum impulse imparted to the newborn NS during the SN event. In a seminal paper, Lyne and Lorimer (1994) showed that radio pulsars receive substantial natal kicks, with mean velocities around $\sim 450 \pm 90 \text{ km s}^{-1}$, based on measurements of their peculiar motions relative to the local standard of rest. This was followed up by Hobbs et al. (2005), and more recently, among others, by Verbunt et al. (2017) and Igoshev (2020).

The origin of pulsar velocities remains under debate. Proposed explanations include asymmetric mass ejection driven by hydrodynamic instabilities during the SN explosion (Janka, 2017); anisotropic neutrino emission influenced by strong magnetic fields (Chugai, 1984; Arras and Lai, 1999); and the so-called ‘electromagnetic rocket’ effect resulting from an off-centre dipolar magnetic field (Harrison and Tademaru, 1975; Agalianou and Gourgouliatos, 2023). In recent years, natal kicks with large amplitudes have been successfully reproduced in 3D SN simulations (e.g. Burrows et al., 2024) which, lately, also try to explain an observed correlation between the NS spin and velocity vectors (see e.g. Johnston et al., 2007; Yao et al., 2021; Janka et al., 2022).

Both theoretical and observational evidence suggests that natal kick amplitudes depend on the NS’s formation pathway. Theoretically, electron-capture SN models predict kicks of less than 10 km s^{-1} (Gessner and Janka, 2018). In tight binaries, where an ultra-stripped SN forms the second-born NS, models indicate that the minimal mass loss involved often (but not always) results in weak natal kicks (Tauris et al., 2015b). Observationally, small kicks are supported by the presence of large

populations of radio pulsars in globular clusters,⁹ which have escape velocities below 50 km s^{-1} . Similarly, small NS kicks are invoked to explain the overabundance of r -process elements in ultra-faint dwarf galaxies, which have even lower escape velocities of $\sim 15 \text{ km s}^{-1}$, as a result of binary NS mergers (e.g. [Ding et al., 2024](#), and references therein). One of the best pieces of evidence for the existence of small kicks is the measured low transverse velocity of the double pulsar with a velocity of $11.1 \pm 1.0 \text{ km s}^{-1}$ and the very small inclination angle between the pulsar spin and the total orbital angular momentum vector of less than 3.2 deg ([Kramer et al., 2021](#)). Conversely, large kicks are required to explain young pulsars — along with their associated bow shocks in SN remnants — moving at velocities exceeding 1000 km s^{-1} (e.g. [Cordes et al., 1993](#); [Schinzel et al., 2019](#)). While it is therefore likely that kick magnitudes are linked to the final structure of the progenitor star and the nature of the SN explosion, the detailed mechanisms remain uncertain.

The main technique for constraining the peculiar velocity — and thus the natal kick — of an individual radio pulsar involves combining a proper motion measurement with either a direct distance measurement (via geometric parallax) or a model-dependent distance estimate based on dispersion measure (DM). Proper motion and parallax can be obtained through either pulsar timing or interferometric imaging. For MSPs, proper motion can be measured to high precision even with a modest timing baseline. Non-recycled pulsars observed over many years can also yield meaningful proper motion constraints ([Hobbs et al., 2004, 2005](#)), although these are often affected by significant uncertainties due to spin noise modelling ([Parthasarathy et al., 2019](#)). Direct distance constraints via timing parallax are typically limited to well-timed recycled pulsars. For most systems, distances are therefore estimated from DM combined with a Galactic electron density model, though this method has limited precision. The resulting distance uncertainties translate into substantial systematic errors in transverse velocity estimates for individual pulsars. Recently, [Ronchi et al. \(2021\)](#) proposed a machine learning approach to infer the characteristic dispersion of a Maxwellian natal kick distribution using only proper motion measurements. Measuring proper motions for ~ 2000 NSs with the SKAO telescopes would allow this method to constrain the underlying velocity dispersion with an uncertainty of approximately 60 km s^{-1} .

High angular resolution interferometric imaging, in contrast to pulsar timing, can provide model-independent distance measurements and thus precise transverse velocity estimates for both recycled and non-recycled pulsars. Approximately 100 such measurements are currently available, with the majority obtained in recent decades through programs using the Very Long Baseline Array (VLBA), such as PSR π ([Deller et al., 2019](#)). This work showed that distances inferred from electron density models — such as NE2001 ([Cordes and Lazio, 2002](#)) and YMW16 ([Yao et al., 2017](#)) — can differ by factors of 3–5 compared to those derived from VLBI parallax measurements. VLBI measurements of parallax and proper motion have been used to constrain the distribution of natal kicks ([Verbunt et al., 2017](#); [Igoshev, 2020](#)). The maximum likelihood techniques employed in these studies favour a bimodal velocity distribution, which can account for both fast and slow kicks. However, it remains unclear whether these two modes correspond to distinct physical mechanisms underlying natal kicks. Additional parallax and proper motion measurements are needed to refine these models and better connect them to the physics of SN explosions.

⁹<https://www3.mpi-fr-bonn.mpg.de/staff/pfreire/GCpsr.html>

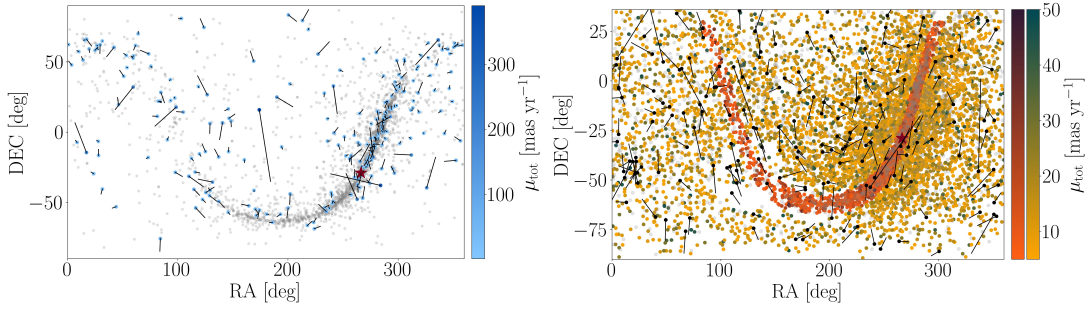


Figure 6: Proper motions of radio pulsars. Top panel: All measured proper motions for standard radio pulsars listed in the ATNF Pulsar Catalogue v2.5.1; Manchester et al. (2005). Bottom panel: Proper motions expected to be measured via timing with SKAO AA*. The simulation corresponds to one realisation of Survey Option 3 with the evolutionary framework outlined in Keane et al. (2025); the corresponding $P-\dot{P}$ diagram is shown in the left panel of Figure 3. Grey dots indicate radio pulsars with $\mu_{\text{tot}} < 5 \text{ mas yr}^{-1}$, which will likely remain undetected by the SKA. Sources with larger proper motions are shown as coloured points according to the respective colour bars. We also show proper motion tracks extrapolated for the past 0.5 Myr. However, only the fastest pulsars with total proper motion $\mu_{\text{tot}} > 50 \text{ mas yr}^{-1}$ are highlighted with black lines in the bottom panel to reduce visual crowding.

The SKAO telescopes will enable proper motion measurements for a large number of pulsars in the southern sky using pulsar timing techniques (see example in Figure 6). In addition, the SKAO will be integrated into VLBI networks to provide precise parallax and proper motion measurements for tens of radio pulsars in the southern hemisphere. These data will offer new constraints on the interstellar medium and contribute to refining the electron density model of the Milky Way.

10 Long-period pulsars

Until the late 2010s, the spin distribution of the observed isolated pulsar population ranged from tens of milliseconds for young systems up to around 10 s for the most magnetic NSs. As outlined in Section 5, pulsar rotation periods in this range are relatively well understood as they are governed by the stars’ initial spin periods and natal magnetic fields, and subsequent spin-down emission and magnetic field evolution (Bates et al., 2014; Gullón et al., 2014, 2015; Cieřlar et al., 2020; Graber et al., 2024). The upper limit in the period distribution has often been interpreted as the result of a highly resistive NS crust accelerating the field decay for stronger fields (Pons et al., 2013). However, given recent advances in search methods in the radio data from single dish and interferometric surveys, several slower, periodic, coherent and highly polarized signals have been discovered. In particular, three radio pulsars, PSR J1903+0433 (Han et al., 2021), PSR J0250+5854 (Tan et al., 2018), and PSR J0901–4046 (Caleb et al., 2022) have been found to rotate at periods of 14 s, 23 s and 76 s, respectively. While the former two sources could be accommodated within current model uncertainties, the discovery of a 76-second radio-loud pulsar began to challenge our understanding of isolated pulsar physics. On the one hand, it is unclear how isolated sources can attain periods $\gtrsim 50 \text{ s}$ questioning current models of magneto-rotational evolution without invoking ad-hoc configurations of core-dominated magnetic fields. On the other hand, based on our existing knowledge of magnetospheric pair production and radio pulsar death lines, PSR J0901-4046’s

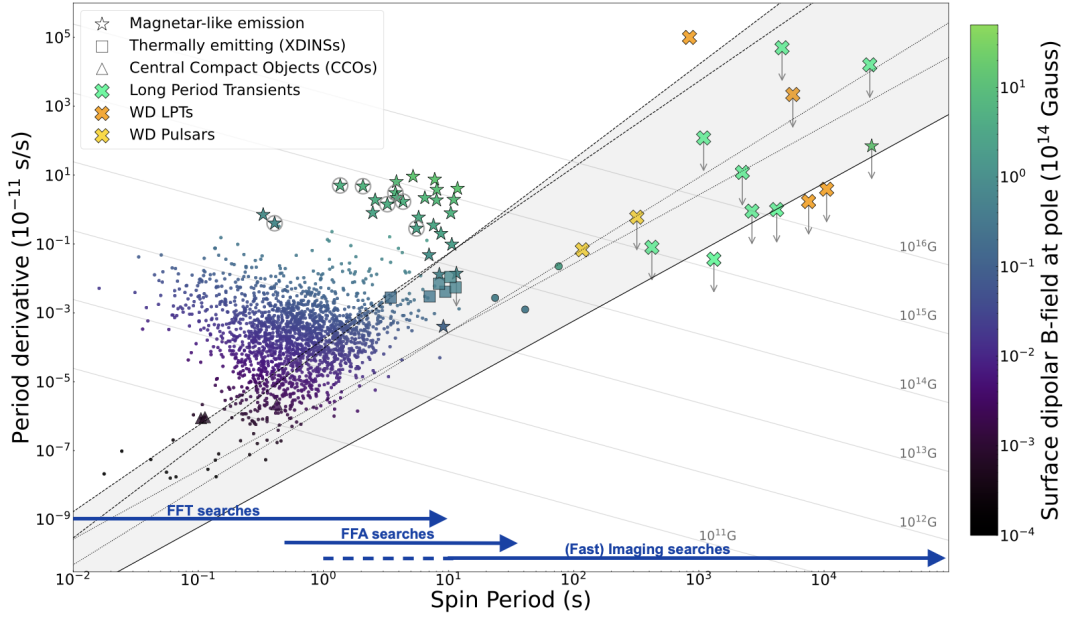


Figure 7: Period-period derivative diagram showing different classes of isolated NSs and known long-period transients, including white-dwarf (WD) pulsars and transients. Adapted from Figure 3 in Rea et al. (2026). The grey circles label the radio magnetars, and the rightmost star is the CCO in RCW103, which has exhibited a magnetar outburst (Rea et al., 2016). The grey region represents possible pulsar emission death lines based on various models (Wang et al., 2025), with the upper limit representing a pure dipole model and the lower one showing a multipole model which is a factor of 10 stronger than the dipole. The blue arrows at the bottom of the plot show approximate pulse period ranges for different search software approaches, see Section 11.1.2. In addition to these, single pulse searches in the time-domain could detect individual pulses from the entire period range, depending on pulse width.

radio-loud nature is difficult to reconcile with standard emission models (Zhang et al., 2000; Chen and Ruderman, 1993; Suvorov and Melatos, 2023).

In recent years, both these issues have been further stretched by the discovery of several new radio sources with even longer spin periods (\gg a few tens of seconds). As illustrated in Figure 7, to date, nine long-period transients have been discovered, with periods ranging between a few minutes to several hours. Most of these objects show transient radio activity, during which bursts with peak flux densities of ~ 1 mJy–50 Jy appear periodically, with duty cycles ranging from ~ 0.01 –30%. In one case, the periodic radio emission has been observed continuously for about 30 years (GPM J1839–10; Hurley-Walker et al. 2023). In two systems, optical observations have identified the presence of a binary white dwarf system with an M-class star with a synchronized spin-orbit (ILT J1101+5521 and GLEAM-X J0704–36; de Ruiter et al. 2025; Hurley-Walker et al. 2024; Rodriguez 2025). For another source, transient X-ray emission has been detected during enhanced radio periodic activity (Wang et al., 2025). The radio emission in these sources shares many similarities with what is seen from radio pulsars (in particular, the high degree of linear polarization and the microstructures) and radio-emitting magnetars (see Section 2) possibly suggesting that at least some of the long-period sources have a NS origin.

Given the full range of observational properties, the nature of long-period radio transients might well be diverse, and the new class might not be composed entirely of NSs. A significant fraction might be a peculiar evolutionary stage of binary white dwarfs potentially related to radio-emitting white-dwarf systems such as AR Sco (Marsh et al., 2016) and J1912–4410 (Pelisoli et al., 2023), or accreting magnetic cataclysmic variables (Schreiber et al., 2021). As we do not observe any radio pulsations from isolated white dwarfs (Pelisoli et al., 2024) (despite many magnetic white dwarfs having periods in the observed range; Rea et al. 2024), the presence of a companion to produce the observed radio emission might be key for this scenario (Buckley et al., 2017). However, given the discovery of PSR J0901–4046 (Caleb et al., 2022), which is difficult to explain in the white-dwarf context, several of the newly discovered long-period sources may indeed be radio-emitting NSs. While angular momentum transfer from a fall-back accretion disk (Chatterjee et al., 2000; Ho and Andersson, 2017; Janka et al., 2022) could, in principle, provide a viable solution for driving significant spin-down in those NSs with the strongest magnetic fields (Ronchi et al., 2022), recent population analyses (e.g. Rea et al., 2024) suggest that the discovery rate of long-period sources in the NS-scenario alone cannot be easily reconciled with the fiducial Galactic core-collapse supernova rate of ~ 2 (Rozwadowska et al., 2021). In addition, the issue of radio pulsar emission at such long periods remains an open problem.

Despite several unanswered questions, the recent discovery of numerous long-period radio transients clearly indicates that previous time-domain radio surveys have been biased against a population of long-period NSs because they were not expected to be radio-loud. High-precision radio monitoring and repeated radio surveys with the SKAO telescopes, combined with multi-wavelength observations, will be key to further exploring the distribution of long-period sources and their underlying nature. First, these studies will provide the most sensitive probes of the evolution of isolated NSs in our Galaxy, allowing us to examine the radio emission from objects close to the pulsar death valley and test the limits of theories of coherent radio emission (Zhang et al., 2000; Chen and Ruderman, 1993; Suvorov and Melatos, 2023). In addition, the unprecedented sensitivity of the SKAO telescopes may enable us to detect very faint radio emission from known radio-quiet X-ray pulsars, RRATs, or new intermittent LPTs where the radio emission may be quenched by the interaction with circumpulsar matter, such as the disks in the fallback disk evolutionary scenario. Monitoring for radio state changes and timing of these faint radio signals could then enable more inferences about the surrounding matter such as the clumpiness of a disk by measuring the torque variability in a precession signature. Finally, detection of X-ray or optical counterparts to these long-period transients will enable us to constrain models of the NS’s magneto-rotational evolution. These aspects will ultimately have significant implications on the yield of pulsars with the SKAO.

11 Observing modes and forecasts for SKAO array assemblies AA* and AA4

Observations of NSs with the SKAO have great potential to significantly advance our understanding of all the different types of sources that have been discussed here, all across the NS family. The SKAO telescopes will be rolled out in so called Array Assemblies (AA), with the currently funded telescopes called AA* and the full design baseline called AA4. For SKA-Mid, AA* will consist of a total of 144 dishes (80 x 15 m diameter and 64 x 13.5 m diameter) with a maximum base line of

36 km, and AA4 will consist of 197 dishes (133 x 15 m diameter and 64 x 13.5 m diameter) with a maximum baseline of 150 km. For SKA-Low, AA* will consist of a total of 307 stations x 256 antennas, with a maximum base line of 74 km, and AA4 will consist of 512 stations x 256 antennas, also with a maximum baseline of 74 km. Further details can be found online¹⁰.

Both SKA-Mid and SKA-Low will be able to perform both pulsar search and pulsar timing, with a range of observing options and data products available. To maximise the scientific output, it will be essential to both find new sources in our Galaxy (and beyond) using the pulsar and single pulse search capabilities, and to set up an efficient pulsar timing programme to follow-up on new and previously known NSs using the pulsar timing capabilities. We outline below suggestions for how a pulsar survey could be set up, with forecasts for both isolated ordinary pulsars and for millisecond pulsars. We then discuss how to optimally set up a pulsar timing programme of known sources.

11.1 Pulsar searches with AA* and AA4

The pulsar search backend will be capable of searching for pulsars and fast transients in (quasi-)real time at both SKAO telescope sites. To get an estimate of the numbers of pulsars that may be detected with each telescope in the two Array Assemblies, we have run simulations both in snapshot mode using PsrPopPy¹¹ (Bates et al., 2014) and in evolutionary mode following the methods described in Graber et al. (2024) and Pardo-Araujo et al. (2025). The details of these simulations can be found in Keane et al. (2026) as part of this special issue. A pulsar survey can be designed and optimised in a variety of ways, with different yields as outcome. One example from Keane et al. (2026) shows that in a composite all-sky survey with SKA-Mid Band 2 focussing on the Galactic plane up to a Galactic latitude of 5° and SKA-Low covering the rest of the visible sky, the detected pulsar population would yield approximately 10,000 ordinary pulsars and 800 MSPs for AA*. The corresponding AA4 detection values are around 12,000 ordinary pulsars and 1,000 MSPs.

Thanks to the many simultaneous beams available in pulsar search mode, all these sources will be well localised instantly, which will in turn enable rapid follow-up with the SKAO telescopes and with other facilities both in the radio domain and in other wavelengths.

11.1.1 Millisecond and binary pulsar surveys

Currently, there are about 550 MSPs known in the Galactic field¹² (and an additional 345 pulsars in 45 Globular Clusters¹³ at the time of writing). This number has grown rapidly over the last 10 years: the total number is three times higher than what was recorded in the 2015 SKA Science book (Tauris et al., 2015a). Our simulations suggest that surveys with the SKAO telescopes should be able to increase the number of MSPs in the Galactic field to ~800 pulsars as part of AA* and ~1000 pulsars in AA4 (Keane et al., 2025).

Many of the known MSPs are in binary systems, which enables a wide range of scientific studies, but also makes them more difficult to detect in the first place. The detectability of these pulsars degrades

¹⁰<https://www.skao.int/en/science-users/646/year-life-ska>

¹¹<https://github.com/samb8s/PsrPopPy>

¹²<https://www.astro.umd.edu/~eferrara/GalacticMSPs.html>

¹³<https://www3.mpifr-bonn.mpg.de/staff/pfreire/GCpsr.html>

due to the orbital acceleration, and computationally intensive acceleration searches, such as those planned with the SKAO telescopes, are needed to detect them. With higher telescope sensitivity, shorter parts of the orbit can be sampled and still result in a detection, and hence some of the currently undetected MSP binary systems will be detectable with the SKAO telescopes. In general, acceleration searches are able to detect pulsars where the integration time is $\lesssim 10\%$ of the binary orbit, if the instantaneous sensitivity is high enough. There are many different combinations of search parameters, observation set-up, and strategy for how to best discover new binary pulsars with both SKA-Mid and SKA-Low - too many to include in this chapter, especially when also considering targeted searches. Some different options are discussed in greater detail in other chapters in this series, please see [Bagchi et al. \(2026\)](#) for searches of Globular Clusters and [Krishnan et al. \(2026\)](#) for searches for binary systems useful for testing theories of gravity. Some of the sources discovered with the SKAO telescopes will be bright enough to follow-up with other radio telescopes, however it is likely that most sources will require the SKAO telescopes sensitivity to monitor them efficiently.

As discussed in section 6, many MSPs have been discovered by targeting unidentified Fermi γ -ray sources. In the future, additional targets may be found through collaborations with other instruments. [Korol et al. \(2024\)](#) modelled the detectability of NS–white dwarf binaries with Laser Interferometer Space Antenna (LISA). They concluded that about 10^2 NS–white dwarf binaries with short orbital periods (< 3 hours) can be discovered by LISA. A significant fraction of these sources are formed with NS recycling, i.e., the NS is a millisecond radio pulsar. The SKAO telescopes could detect some of these MSPs as a follow-up from a LISA discovery.

11.1.2 Additional thoughts on surveys for long-period pulsars

The SKAO telescopes could remove the observational selection bias for radio pulsation periods of more than a few seconds with respect to detecting and regular monitoring.

Different observation and search techniques are required for discovering pulsars in different period ranges, see Figure 7. Most commonly, an FFT search is carried out for periods up to ~ 10 seconds, and such a search will be carried out with the SKAO pulsar search backends. For finding sources with periods longer than that, at the lower end of the long-period pulsar range, the use of a Fast Folding Algorithm (FFA) running on the pulsar survey data would be highly beneficial. An FFA search is more sensitive than traditional FFT searches, in particular in the case of long-period pulsars (e.g. [Morello et al., 2020](#)). Running an FFA on the entire periodicity search range would be computationally expensive, but may be feasible by limiting the parameter space to the longest periods and would be an excellent addition to the pulsar search backend in the future.

One of the key challenges to finding pulsars with long periods is the presence of red noise, due to the varying baseline of the time series. Techniques like subtraction of the incoherent beam power from each tied array beam would be highly advantageous in reducing the adverse effects of red noise when searching for long-period sources in particular, see [Roy et al. \(2018\)](#) for incoherent beam subtraction and application to the GMRT telescope.

Furthermore, searching for transient radio emission in radio images at higher time resolution will allow for more and longer period discoveries. Along with single pulse searches in the time-domain, a fast imaging search is a proven technique for finding sources with long periods. Such searches

have been carried out very successfully at various telescopes in the recent years, e.g. the GLEAM-X survey with the MWA (Hurley-Walker et al., 2022), ThunderKAT with the MeerKAT telescope (Fender et al., 2016), and in searches with the ASKAP telescope (e.g. Caleb et al., 2024). In the case of the SKAO, this will be made possible by use of the Fast Imaging Pipelines at each telescope, which are planned to search for transients with a time scale of as short as 1 second in the fast-imaging products.

In addition to these techniques, single pulse searches of time-domain data, such as those used in FRB surveys, are also used to search for pulsars over the entire period range. See e.g. Caleb et al. (2026) and other papers from the SKAO Transients working group (Miller-Jones et al., 2026) for extended discussion on searches for single pulses of radio emission.

11.2 Pulsar timing modes and regular monitoring

To enable all the science cases mentioned, it is not only necessary to find a large number of NSs, but all these sources also need to be monitored with pulsar timing to reveal their properties. With the large numbers of NS discoveries that are anticipated from the SKAO telescopes, it is essential to design an efficient strategy for follow-up observations and continuous monitoring of these pulsars. Some of the new discoveries may still be possible to observe with other radio telescopes, and collaboration between the SKAO and other radio telescopes should be highly encouraged, but many of the new sources are expected to fall below the detection threshold at many other facilities. To enable the science as discussed in this chapter, it is also crucial to regularly monitor many of the currently known NSs in addition to the new discoveries.

For this to be feasible, it will be vital to make use of the multibeaming capability of the Pulsar Timing backend in combination with efficient use of telescope subarrays. A similar approach has been taken at the MeerKAT telescope over the last few years, through the Thousand Pulsar Array (TPA, Johnston et al., 2020)¹⁴ as part of the MeerTime project. The TPA was set up to regularly monitor at least 500 ordinary pulsars for a period of 5 years, and to obtain polarised pulse profiles for an additional 500 pulsars. The observation strategy is described in Song et al. (2021), and discusses how the overall observing time can be reduced by the optimal use of MeerKAT’s subarray capabilities. The TPA project’s observation strategy first calculates the required integration length to reach a high-fidelity profile for each pulsar. It then compares the ratios of system noise to pulse-to-pulse variability to determine if subarraying would be beneficial if used for that particular pulsar. Song et al. (2021) also presents an example of observing 1000 pulsars with SKA-Mid, and shows that significant reductions in observing time can be achieved with careful consideration of subarrays. They find the highest time savings by allowing the 1000 pulsars to be observed in subarrays of different sizes, but fixed within an observing session. A similar analysis, using the latest array and telescope configurations for the various array assemblies, should be carried out closer to the start of SKAO operations to ensure optimal use of telescope time.

Another aspect of ensuring efficiency of telescope time is the use of ‘filler time’. Especially at the SKA-Low telescope, where other science goals at times may be restricted by e.g. the sun or the moon, short pulsar timing observations could be added in gaps in the schedule. It is also important

¹⁴<http://www.meertime.org/1000-pulsar-array.html>

to consider commensal observations where possible, as many sources may not need the full array or a large amount of computing resources. Making use of all these capabilities will help ensure the success of pulsar timing projects with the SKAO telescopes.

All these data, gathered with SKA-Low and SKA-Mid, will help us to study the different characteristics of radio-emitting neutron stars. These can be contrasted and compared to find differences and similarities. This will not only provide important insights into the emission processes of various types (e.g. Kramer et al., 2024), but also shed light on potential evolutionary pathways connecting the different manifestations of NSs. This will help us to understand not only the specific sub-population, but also the aforementioned birth rate problem. A complete NS census with the SKA promises to provide a holistic view of NSs in the Milky Way and beyond.

Acknowledgments

We thank Aru Beri, Paolo Esposito, Fabian Jankowski, and Danny Vohl for helpful comments. V. G. is supported by a UKRI Future Leaders Fellowship (grant number MR/Y018257/1). N.R. is supported by the European Research Council (ERC CoG No. 817661 and ERC PoC No. 101189496), and grants SGR2021-01269, ID2023-153099NA-I00, and CEX2020-001058-M.

References

- A. Abac et al. *arXiv e-prints*, art. arXiv:2503.12263, Mar. 2025a. doi: 10.48550/arXiv.2503.12263.
- A. G. Abac et al. *ApJ*, 983(2):99, Apr. 2025b. doi: 10.3847/1538-4357/adb3a0.
- F. Abbate et al. In *Advancing Astrophysics with the SKA – II (AASKAII)*. 2026. arXiv search: Report number AASKAII/Abbate01.
- B. P. Abbott et al. *Phys. Rev. L.*, 119(16):161101, Oct. 2017. doi: 10.1103/PhysRevLett.119.161101.
- B. P. Abbott et al. *ApJL*, 892(1):L3, Mar. 2020a. doi: 10.3847/2041-8213/ab75f5.
- R. Abbott et al. *ApJL*, 896(2):L44, June 2020b. doi: 10.3847/2041-8213/ab960f.
- A. A. Abdo et al. *Science*, 325(5942):848, Aug. 2009. doi: 10.1126/science.1176113.
- Abhishek et al. *JAA*, 43(2):75, Dec. 2022. doi: 10.1007/s12036-022-09862-3.
- V. Agaljanou and K. N. Gourgouliatos. *MNRAS*, 522(4):5879–5891, July 2023. doi: 10.1093/mnras/stad1344.
- D. Agarwal et al. *MNRAS*, 549(1):stag787, June 2026. doi: 10.1093/mnras/stag787.
- D. N. Aguilera, J. A. Pons, and J. A. Miralles. *ApJL*, 673(2):L167, Feb. 2008. doi: 10.1086/527547.
- M. Ajello et al. *ApJ*, 861(2):85, Jul 2018. doi: 10.3847/1538-4357/aac515.
- J. A. J. Alford and J. P. Halpern. *ApJ*, 944(1):36, Feb. 2023. doi: 10.3847/1538-4357/acaf55.
- M. A. Alpar, A. F. Cheng, M. A. Ruderman, and J. Shaham. *Nature*, 300(5894):728–730, Dec. 1982. doi: 10.1038/300728a0.
- B. C. Andersen and S. M. Ransom. *ApJL*, 863(1):L13, Aug. 2018. doi: 10.3847/2041-8213/aad59f.
- L. D. Anderson et al. *A&A*, 605:A58, 9 2017. ISSN 0004-6361. doi: 10.1051/0004-6361/201731019. URL <http://www.aanda.org/10.1051/0004-6361/201731019>.
- J. Antoniadis. *MNRAS*, 501(1):1116–1126, Feb. 2021. doi: 10.1093/mnras/staa3595.
- J. Antoniadis et al. *ApJ*, 830(1):36, Oct. 2016. doi: 10.3847/0004-637X/830/1/36.
- A. M. Archibald et al. *Science*, 324(5933):1411, June 2009. doi: 10.1126/science.1172740.

- R. F. Archibald, V. M. Kaspi, S. P. Tendulkar, and P. Scholz. *ApJL*, 829(1):L21, Sept. 2016. doi: 10.3847/2041-8205/829/1/L21.
- P. Arras and D. Lai. *ApJ*, 519(2):745–749, July 1999. doi: 10.1086/307407.
- S. Ascenzi et al. *MNRAS*, 533(1):201–224, Sept. 2024. doi: 10.1093/mnras/stae1749.
- M. Bagchi, D. R. Lorimer, and S. Wolfe. *MNRAS*, 432(2):1303–1314, June 2013. doi: 10.1093/mnras/stt559.
- M. Bagchi et al. In *Advancing Astrophysics with the SKA – II (AASKAII)*. 2026. arXiv search: Report number AASKAII/Bagchi01.
- J. Bai et al. *ApJ*, 979(2):122, Feb. 2025. doi: 10.3847/1538-4357/ada3c4.
- V. Balakrishnan et al. *MNRAS*, 511(1):1265–1284, Mar. 2022. doi: 10.1093/mnras/stab3746.
- E. Barr. Peasoup: C++/CUDA GPU pulsar searching library. Astrophysics Source Code Library, record ascl:2001.014, Jan. 2020.
- E. D. Barr et al. *MNRAS*, 465(2):1711–1719, Feb. 2017. doi: 10.1093/mnras/stw2947.
- E. D. Barr et al. *Science*, 383(6680):275–279, Jan. 2024. doi: 10.1126/science.adg3005.
- A. Basu et al. Probing neutron star interiors and the properties of cold, ultra-dense matter with the SKA. Submitted, 2025.
- A. Basu et al. In *Advancing Astrophysics with the SKA – II (AASKAII)*. 2026. arXiv search: Report number AASKAII/AvishekBasu01.
- S. D. Bates, D. R. Lorimer, A. Rane, and J. Swiggum. *MNRAS*, 439(3):2893–2902, Apr. 2014. doi: 10.1093/mnras/stu157.
- K. Belczynski et al. *ApJSS*, 174(1):223–260, Jan. 2008. doi: 10.1086/521026.
- O. G. Benvenuto, M. A. De Vito, and J. E. Horvath. *ApJL*, 786(1):L7, May 2014. doi: 10.1088/2041-8205/786/1/L7.
- D. Bhattacharya and E. P. J. van den Heuvel. *Phys. Rep.*, 203(1-2):1–124, Jan. 1991. doi: 10.1016/0370-1573(91)90064-S.
- C. D. Bochenek et al. *Nature*, 587(7832):59–62, Nov. 2020. doi: 10.1038/s41586-020-2872-x.
- D. A. H. Buckley et al. *Nature Astronomy*, 1:0029, Jan. 2017. doi: 10.1038/s41550-016-0029.
- M. Burgay et al. *Nature*, 426(6966):531–533, Dec. 2003. doi: 10.1038/nature02124.
- S. Burke-Spolaor. In J. van Leeuwen, editor, *Neutron Stars and Pulsars: Challenges and Opportunities after 80 years*, volume 291 of *IAU Symposium*, pages 95–100, Mar. 2013. doi: 10.1017/S1743921312023277.
- A. Burrows, T. Wang, D. Vartanyan, and M. S. B. Coleman. *ApJ*, 963(1):63, Mar. 2024. doi: 10.3847/1538-4357/ad2353.
- M. Caleb et al. *Nature Astronomy*, 6:828–836, May 2022. doi: 10.1038/s41550-022-01688-x.
- M. Caleb et al. *Nature Astronomy*, 8:1159–1168, Sept. 2024. doi: 10.1038/s41550-024-02277-w.
- M. Caleb et al. In *Advancing Astrophysics with the SKA – II (AASKAII)*. 2026. arXiv search: Report number AASKAII/Caleb02.
- F. Camilo et al. *ApJ*, 746(1):63, Feb. 2012. doi: 10.1088/0004-637X/746/1/63.
- D. J. Champion et al. *Science*, 320(5881):1309, June 2008. doi: 10.1126/science.1157580.
- P. Chatterjee, L. Hernquist, and R. Narayan. *ApJ*, 534(1):373–379, May 2000. doi: 10.1086/308748.
- D. Chattopadhyay et al. *MNRAS*, 504(3):3682–3710, July 2021. doi: 10.1093/mnras/stab973.
- H.-L. Chen, X. Chen, T. M. Tauris, and Z. Han. *ApJ*, 775(1):27, Sept. 2013. doi: 10.1088/0004-637X/775/1/27.

- K. Chen and M. Ruderman. *ApJ*, 402:264, Jan. 1993. doi: 10.1086/172129.
- CHIME/FRB Collaboration et al. *Nature*, 587(7832):54–58, Nov. 2020. doi: 10.1038/s41586-020-2863-y.
- N. N. Chugai. *Soviet Astronomy Letters*, 10:87, Feb. 1984.
- M. Cieřlar, T. Bulik, and S. Osłowski. *MNRAS*, 492(3):4043–4057, Mar. 2020. doi: 10.1093/mnras/staa073.
- C. J. Clark et al. *Nature Astronomy*, 7:451–462, Apr. 2023. doi: 10.1038/s41550-022-01874-x.
- J. M. Cordes and T. J. W. Lazio. *arXiv e-prints*, art. astro-ph/0207156, July 2002. doi: 10.48550/arXiv.astro-ph/0207156.
- J. M. Cordes, R. W. Romani, and S. C. Lundgren. *Nature*, 362(6416):133–135, Mar. 1993. doi: 10.1038/362133a0.
- J. M. Cordes et al. *New Astronomy Reviews*, 48(11-12):1413–1438, Dec. 2004. doi: 10.1016/j.newar.2004.09.040.
- M. Cruces, A. Reisenegger, and T. M. Tauris. *MNRAS*, 490(2):2013–2022, Dec. 2019. doi: 10.1093/mnras/stz2701.
- M. Cruise et al. *Nature Astronomy*, 9:36–44, Jan. 2025. doi: 10.1038/s41550-024-02416-3.
- B. Y. Cui, J. Boyles, M. A. McLaughlin, and N. Palliyaguru. *ApJ*, 840(1):5, May 2017. doi: 10.3847/1538-4357/aa6aa9.
- T. Damour and J. H. Taylor. *Phys. Rev. D*, 45(6):1840–1868, Mar. 1992. doi: 10.1103/PhysRevD.45.1840.
- D. De Grandis et al. *ApJ*, 903(1):40, Nov. 2020. doi: 10.3847/1538-4357/abb6f9.
- A. De Luca. In *Journal of Physics Conference Series*, volume 932 of *Journal of Physics Conference Series*, page 012006. IOP, Dec. 2017. doi: 10.1088/1742-6596/932/1/012006.
- I. de Ruiter et al. *Nature Astronomy*, 9:672–684, May 2025. doi: 10.1038/s41550-025-02491-0.
- J. Debnath, M. Bagchi, and A. Basu. *MNRAS*, 524(4):5411–5431, Oct. 2023. doi: 10.1093/mnras/stad2147.
- C. Dehman et al. *MNRAS*, 523(4):5198–5206, Aug. 2023a. doi: 10.1093/mnras/stad1773.
- C. Dehman, D. Viganò, J. A. Pons, and N. Rea. *MNRAS*, 518(1):1222–1242, Jan. 2023b. doi: 10.1093/mnras/stac2761.
- A. J. Delgado and H.-C. Thomas. *A&A*, 96(1-2):142–145, Mar. 1981.
- A. T. Deller et al. *ApJ*, 875(2):100, Apr. 2019. doi: 10.3847/1538-4357/ab11c7.
- J. S. Deneva et al. *ApJ*, 775(1):51, Sept. 2013. doi: 10.1088/0004-637X/775/1/51.
- H. Ding et al. *ApJ*, 970(1):90, July 2024. doi: 10.3847/1538-4357/ad4883.
- L. Dirson, J. Pétri, and D. Mitra. *A&A*, 667:A82, Nov. 2022. doi: 10.1051/0004-6361/202243305.
- R. Dokara et al. *A&A*, 651:A86, 7 2021. ISSN 0004-6361. doi: 10.1051/0004-6361/202039873. URL <https://www.aanda.org/10.1051/0004-6361/202039873>.
- O. V. Doroshenko and S. M. Kopeikin. *MNRAS*, 274(4):1029–1038, June 1995. doi: 10.1093/mnras/274.4.1029.
- V. Doroshenko, V. Suleimanov, G. Pühlhofer, and A. Santangelo. *Nature Astronomy*, 6:1444–1451, Dec. 2022. doi: 10.1038/s41550-022-01800-1.
- S.-S. Du et al. *ApJ*, 968(2):105, June 2024. doi: 10.3847/1538-4357/ad4450.
- R. C. Duncan and C. Thompson. *ApJL*, 392:L9, June 1992. doi: 10.1086/186413.
- C. M. Espinoza et al. *ApJL*, 741(1):L13, Nov. 2011. doi: 10.1088/2041-8205/741/1/L13.

- C. M. Espinoza, A. G. Lyne, and B. W. Stappers. *MNRAS*, 466(1):147–162, Apr. 2017. doi: 10.1093/mnras/stw3081.
- C.-A. Faucher-Giguère and V. M. Kaspi. *ApJ*, 643(1):332–355, May 2006. doi: 10.1086/501516.
- R. Fender et al. In *MeerKAT Science: On the Pathway to the SKA*, page 13, Jan. 2016. doi: 10.22323/1.277.0013.
- G. Ferrand and S. Safi-Harb. *Advances in Space Research*, 49(9):1313–1319, May 2012. doi: 10.1016/j.asr.2012.02.004.
- E. Fonseca et al. *Astrophys. J. Lett.*, 915(1):L12, 2021. doi: 10.3847/2041-8213/ac03b8.
- P. C. C. Freire and N. Wex. *Living Reviews in Relativity*, 27(1):5, Dec. 2024. doi: 10.1007/s41114-024-00051-y.
- P. C. C. Freire et al. *MNRAS*, 412(4):2763–2780, Apr. 2011. doi: 10.1111/j.1365-2966.2010.18109.x.
- B. M. Gaensler, D. C. J. Bock, and B. W. Stappers. *ApJL*, 537(1):L35–L38, July 2000. doi: 10.1086/312750.
- F. P. Gavriil et al. *Science*, 319(5871):1802, Mar. 2008. doi: 10.1126/science.1153465.
- A. A. Gençali and Ü. Ertan. *MNRAS*, 534(2):1481–1489, Oct. 2024. doi: 10.1093/mnras/stae2177.
- A. Gessner and H.-T. Janka. *ApJ*, 865(1):61, Sept. 2018. doi: 10.3847/1538-4357/aadbae.
- E. Gotthelf, K. Perez, and J. Halpern. In *AAS/High Energy Astrophysics Division*, volume 21 of *AAS/High Energy Astrophysics Division*, page 107.47, May 2024.
- E. V. Gotthelf and J. P. Halpern. *ApJ*, 900(2):159, Sept. 2020. doi: 10.3847/1538-4357/aba7bc.
- E. V. Gotthelf, J. P. Halpern, and J. Alford. *ApJ*, 765(1):58, Mar. 2013a. doi: 10.1088/0004-637X/765/1/58.
- E. V. Gotthelf, J. P. Halpern, B. Allen, and B. Knispel. *ApJ*, 773(2):141, Aug. 2013b. doi: 10.1088/0004-637X/773/2/141.
- K. N. Gourgouliaos, T. S. Wood, and R. Hollerbach. *Proceedings of the National Academy of Science*, 113(15):3944–3949, Apr. 2016. doi: 10.1073/pnas.1522363113.
- V. Graber, M. Ronchi, C. Pardo-Araujo, and N. Rea. *ApJ*, 968(1):16, June 2024. doi: 10.3847/1538-4357/ad3e78.
- D. A. Green. A Catalogue of Galactic Supernova Remnants (2022 December version). Cavendish Laboratory, Cambridge, United Kingdom (available at <https://www.mrao.cam.ac.uk/surveys/snrs-2022/>), Accessed: from 2023-01-09, 2022. Accessed: from 2023-01-09.
- K. Grunthal et al. *A&A*, 691:A22, Nov. 2024. doi: 10.1051/0004-6361/202347482.
- M. Gullón, J. A. Miralles, D. Viganò, and J. A. Pons. *MNRAS*, 443(3):1891–1899, Sept. 2014. doi: 10.1093/mnras/stu1253.
- M. Gullón et al. *MNRAS*, 454(1):615–625, Nov. 2015. doi: 10.1093/mnras/stv1644.
- J. E. Gunn and J. P. Ostriker. *ApJ*, 160:979, June 1970. doi: 10.1086/150487.
- J. P. Halpern and E. V. Gotthelf. *ApJ*, 709(1):436–446, Jan. 2010. doi: 10.1088/0004-637X/709/1/436.
- J. L. Han et al. *Research in Astronomy and Astrophysics*, 21(5):107, June 2021. doi: 10.1088/1674-4527/21/5/107.
- E. R. Harrison and E. Tademaru. *ApJ*, 201:447–461, Oct. 1975. doi: 10.1086/153907.
- J. W. T. Hessels et al. *Science*, 311(5769):1901–1904, Mar. 2006. doi: 10.1126/science.1123430.
- W. C. G. Ho. *MNRAS*, 414(3):2567–2575, July 2011. doi: 10.1111/j.1365-2966.2011.18576.x.

- W. C. G. Ho. *MNRAS*, 452(1):845–851, Sept. 2015. doi: 10.1093/mnras/stv1339.
- W. C. G. Ho and N. Andersson. *MNRAS*, 464(1):L65–L69, Jan. 2017. doi: 10.1093/mnras/llw186.
- G. Hobbs et al. *MNRAS*, 353(4):1311–1344, Oct. 2004. doi: 10.1111/j.1365-2966.2004.08157.x.
- G. Hobbs, D. R. Lorimer, A. G. Lyne, and M. Kramer. *MNRAS*, 360(3):974–992, July 2005. doi: 10.1111/j.1365-2966.2005.09087.x.
- H. Hu et al. *A&A*, 667:A149, Nov. 2022. doi: 10.1051/0004-6361/202244825.
- L. Huang, C. Yu, and H. Tong. *ApJ*, 827(1):80, Aug. 2016. doi: 10.3847/0004-637X/827/1/80.
- N. Hurley-Walker et al. *PASA*, 36:e045, 2019. ISSN 1323-3580. doi: 10.1017/pasa.2019.34.
- N. Hurley-Walker et al. *PASA*, 39:e035, Aug. 2022. doi: 10.1017/pasa.2022.17.
- N. Hurley-Walker et al. *Nature*, 619(7970):487–490, July 2023. doi: 10.1038/s41586-023-06202-5.
- N. Hurley-Walker et al. *ApJL*, 976(2):L21, Dec. 2024. doi: 10.3847/2041-8213/ad890e.
- A. Igoshev et al. *Nature Astronomy*, 9:541–551, Apr. 2025. doi: 10.1038/s41550-025-02477-y.
- A. P. Igoshev. *MNRAS*, 494(3):3663–3674, May 2020. doi: 10.1093/mnras/staa958.
- A. P. Igoshev et al. *MNRAS*, 514(3):4606–4619, Aug. 2022. doi: 10.1093/mnras/stac1648.
- H.-T. Janka. *ApJ*, 837(1):84, Mar. 2017. doi: 10.3847/1538-4357/aa618e.
- H.-T. Janka, A. Wongwathanarat, and M. Kramer. *ApJ*, 926(1):9, Feb. 2022. doi: 10.3847/1538-4357/ac403c.
- L. Jiang, T. M. Tauris, W.-C. Chen, and J. Fuller. *ApJL*, 920(2):L36, Oct. 2021. doi: 10.3847/2041-8213/ac2cc9.
- S. Johnston and A. Karastergiou. *MNRAS*, 467(3):3493–3499, May 2017. doi: 10.1093/mnras/stx377.
- S. Johnston et al. *MNRAS*, 381(4):1625–1637, Nov. 2007. doi: 10.1111/j.1365-2966.2007.12352.x.
- S. Johnston et al. *MNRAS*, 493(3):3608–3615, Apr. 2020. doi: 10.1093/mnras/staa516.
- C. Kalapotharakos, D. Kazanas, A. Harding, and I. Contopoulos. *ApJ*, 749(1):2, Apr. 2012. doi: 10.1088/0004-637X/749/1/2.
- V. M. Kaspi. *Proceedings of the National Academy of Science*, 107(16):7147–7152, Apr. 2010. doi: 10.1073/pnas.1000812107.
- V. M. Kaspi and A. M. Beloborodov. *Annual Review of Astronomy and Astrophysics*, 55(1):261–301, Aug. 2017. doi: 10.1146/annurev-astro-081915-023329.
- V. M. Kaspi and M. A. McLaughlin. *ApJL*, 618(1):L41–L44, Jan. 2005. doi: 10.1086/427628.
- E. Keane et al. In *Advancing Astrophysics with the Square Kilometre Array (AASKA14)*, page 40, Apr. 2015. doi: 10.22323/1.215.0040.
- E. F. Keane and M. Kramer. *MNRAS*, 391(4):2009–2016, Dec. 2008. doi: 10.1111/j.1365-2966.2008.14045.x.
- E. F. Keane et al. A Square Kilometre Array Pulsar Census. Submitted, 2025.
- E. F. Keane et al. In *Advancing Astrophysics with the SKA – II (AASKAII)*. 2026. arXiv search: Report number AASKAII/Keane01.
- V. Korol et al. *MNRAS*, 530(1):844–860, May 2024. doi: 10.1093/mnras/stae889.
- M. Kramer et al. *Science*, 312(5773):549–551, Apr. 2006. doi: 10.1126/science.1124060.
- M. Kramer et al. *Physical Review X*, 11(4):041050, Oct. 2021. doi: 10.1103/PhysRevX.11.041050.
- M. Kramer et al. *Nature Astronomy*, 8:230–240, Feb. 2024. doi: 10.1038/s41550-023-02125-3.
- V. V. Krishnan et al. In *Advancing Astrophysics with the SKA – II (AASKAII)*. 2026. arXiv search: Report number AASKAII/VenkatramanKrishnan01.

- M. U. Kruckow et al. *MNRAS*, 481(2):1908–1949, Dec. 2018. doi: 10.1093/mnras/sty2190.
- J. Li, A. Spitkovsky, and A. Tchekhovskoy. *ApJL*, 746(2):L24, Feb. 2012. doi: 10.1088/2041-8205/746/2/L24.
- M. Linares. In *13th Frascati Workshop on Multifrequency Behaviour of High Energy Cosmic Sources*, 10 2019.
- K. Liu, R. P. Eatough, N. Wex, and M. Kramer. *MNRAS*, 445(3):3115–3132, Dec. 2014. doi: 10.1093/mnras/stu1913.
- D. R. Lorimer. In F. Camilo and B. M. Gaensler, editors, *Young Neutron Stars and Their Environments*, volume 218 of *IAU Symposium*, page 105, Jan. 2004. doi: 10.48550/arXiv.astro-ph/0308501.
- D. R. Lorimer et al. *Science*, 318(5851):777, Nov. 2007. doi: 10.1126/science.1147532.
- D. R. Lorimer et al. *ApJ*, 758(2):141, Oct. 2012. doi: 10.1088/0004-637X/758/2/141.
- M. E. Lower et al. *MNRAS*, 508(3):3251–3274, Dec. 2021. doi: 10.1093/mnras/stab2678.
- M. E. Lower et al. *arXiv e-prints*, art. arXiv:2501.03500, Jan. 2025. doi: 10.48550/arXiv.2501.03500.
- W.-J. Lu et al. *ApJ*, 963(2):151, Mar. 2024. doi: 10.3847/1538-4357/ad27cf.
- J. Luo et al. *ApJ*, 808(2):130, Aug. 2015. doi: 10.1088/0004-637X/808/2/130.
- LVK Collaboration et al. *MNRAS*, 524(4):5984–5992, Oct. 2023. doi: 10.1093/mnras/stad588.
- A. Lyne et al. *Science*, 329(5990):408, July 2010. doi: 10.1126/science.1186683.
- A. G. Lyne and D. R. Lorimer. *Nature*, 369(6476):127–129, May 1994. doi: 10.1038/369127a0.
- A. G. Lyne et al. *Science*, 303(5661):1153–1157, Feb. 2004. doi: 10.1126/science.1094645.
- A. G. Lyne et al. *ApJ*, 834(1):72, Jan. 2017. doi: 10.3847/1538-4357/834/1/72.
- R. N. Manchester, G. B. Hobbs, A. Teoh, and M. Hobbs. *AJ*, 129(4):1993–2006, Apr. 2005. doi: 10.1086/428488.
- T. R. Marsh et al. *Nature*, 537(7620):374–377, Sept. 2016. doi: 10.1038/nature18620.
- J. G. Martinez et al. *ApJ*, 812(2):143, Oct. 2015. doi: 10.1088/0004-637X/812/2/143.
- M. A. McLaughlin et al. *Nature*, 439(7078):817–820, Feb. 2006. doi: 10.1038/nature04440.
- M. A. McLaughlin et al. *ApJ*, 670(2):1307–1313, Dec. 2007. doi: 10.1086/522335.
- D. B. Melrose and R. Yuen. *MNRAS*, 437(1):262–272, Jan. 2014. doi: 10.1093/mnras/stt1876.
- A. Merloni et al. *A&A*, 682:A34, Feb. 2024. doi: 10.1051/0004-6361/202347165.
- J. Miller-Jones, K. Rajwade, and P. A. W. J. W. Hessels. In *Advancing Astrophysics with the SKA – II (AASKAII)*. 2026. arXiv search: Report number AASKAII/Miller-Jones01.
- D. Misra, M. Linares, and C. S. Ye. *A&A*, 693:A314, Jan. 2025. doi: 10.1051/0004-6361/202452035.
- V. Morello et al. *MNRAS*, 497(4):4654–4671, Oct. 2020. doi: 10.1093/mnras/staa2291.
- B. Müller, A. Heger, and J. Powell. *Phys. Rev. L.*, 134(7):071403, Feb. 2025. doi: 10.1103/PhysRevLett.134.071403.
- E. M. Novoselov et al. *MNRAS*, 494(3):3899–3911, May 2020. doi: 10.1093/mnras/staa904.
- S. A. Olausen and V. M. Kaspi. *ApJ Supplement Series*, 212(1):6, May 2014. doi: 10.1088/0067-0049/212/1/6.
- L. Oswald et al. In *Advancing Astrophysics with the SKA – II (AASKAII)*. 2026. arXiv search: Report number AASKAII/Oswald01.
- L. S. Oswald et al. Understanding pulsar magnetospheres with the SKAO. Submitted, 2025.

- A. Papitto et al. *Nature*, 501(7468):517–520, Sept. 2013. doi: 10.1038/nature12470.
- C. Pardo-Araujo, M. Ronch, V. Graber, and N. Rea. *A&A*, 696:A114, Apr. 2025. doi: 10.1051/0004-6361/202453314.
- A. Parthasarathy et al. *MNRAS*, 489(3):3810–3826, Nov. 2019. doi: 10.1093/mnras/stz2383.
- G. G. Pavlov, D. Sanwal, and M. A. Teter. In F. Camilo and B. M. Gaensler, editors, *Young Neutron Stars and Their Environments*, volume 218 of *IAU Symposium*, page 239, Jan. 2004. doi: 10.48550/arXiv.astro-ph/0311526.
- I. Pelisoli et al. *Nature Astronomy*, 7:931–942, Aug. 2023. doi: 10.1038/s41550-023-01995-x.
- I. Pelisoli et al. *MNRAS*, 531(1):1805–1822, June 2024. doi: 10.1093/mnras/stae1275.
- A. Philippov, A. Tchekhovskoy, and J. G. Li. *MNRAS*, 441(3):1879–1887, July 2014. doi: 10.1093/mnras/stu591.
- J. A. Pons, D. Viganò, and N. Rea. *Nature Physics*, 9(7):431–434, July 2013. doi: 10.1038/nphys2640.
- S. B. Popov et al. *MNRAS*, 401(4):2675–2686, Feb. 2010. doi: 10.1111/j.1365-2966.2009.15850.x.
- B. Posselt et al. *MNRAS*, 508(3):4249–4268, Dec. 2021. doi: 10.1093/mnras/stab2775.
- B. Posselt et al. *MNRAS*, 520(3):4582–4600, Apr. 2023. doi: 10.1093/mnras/stac3383.
- V. Radhakrishnan and G. Srinivasan. *Current Science*, 51:1096–1099, Dec. 1982.
- R. R. Rafikov and D. Lai. *Phys. Rev. D*, 73(6):063003, Mar. 2006. doi: 10.1103/PhysRevD.73.063003.
- K. M. Rajwade et al. *ApJL*, 985(1):L3, May 2025. doi: 10.3847/2041-8213/add0a8.
- S. Ransom. PRESTO: PulsAR Exploration and Search TOolkit. Astrophysics Source Code Library, record ascl:1107.017, July 2011.
- S. M. Ransom et al. *Science*, 307(5711):892–896, Feb. 2005. doi: 10.1126/science.1108632.
- S. M. Ransom et al. *Nature*, 505(7484):520–524, Jan. 2014. doi: 10.1038/nature12917.
- N. Rea and D. De Grandis. In *Encyclopedia of Astrophysics*, volume 3, pages 205–222, Jan. 2026. doi: 10.1016/B978-0-443-21439-4.00096-1.
- N. Rea et al. *ApJL*, 828(1):L13, Sept. 2016. doi: 10.3847/2041-8205/828/1/L13.
- N. Rea et al. *ApJ*, 961(2):214, Feb. 2024. doi: 10.3847/1538-4357/ad165d.
- N. Rea, N. Hurley-Walker, and M. Caleb. *Journal of High Energy Astrophysics*, 52:100566, Apr. 2026. doi: 10.1016/j.jheap.2026.100566.
- M. Rigoselli et al. *ApJ*, 976(2):228, Dec. 2024. doi: 10.3847/1538-4357/ad8cd6.
- M. S. E. Roberts. In J. van Leeuwen, editor, *Neutron Stars and Pulsars: Challenges and Opportunities after 80 years*, volume 291 of *IAU Symposium*, pages 127–132, Mar. 2013. doi: 10.1017/S174392131202337X.
- A. C. Rodriguez. *A&A*, 695:L8, Mar. 2025. doi: 10.1051/0004-6361/202553684.
- R. W. Romani et al. *ApJL*, 934(2):L17, Aug. 2022. doi: 10.3847/2041-8213/ac8007.
- M. Ronchi et al. *ApJ*, 916(2):100, Aug. 2021. doi: 10.3847/1538-4357/ac05bd.
- M. Ronchi, N. Rea, V. Graber, and N. Hurley-Walker. *ApJ*, 934(2):184, Aug. 2022. doi: 10.3847/1538-4357/ac7cec.
- J. Roy, J. N. Chengalur, and U.-L. Pen. *ApJ*, 864(2):160, Sept. 2018. doi: 10.3847/1538-4357/aad815.
- K. Rozwadowska, F. Vissani, and E. Cappellaro. *New Astronomy*, 83:101498, Feb. 2021. doi: 10.1016/j.newast.2020.101498.

- T. Salmi et al. *ApJ*, 974(2):294, Oct. 2024. doi: 10.3847/1538-4357/ad5f1f.
- M. Sautron et al. *ApJ*, 986(1):88, June 2025. doi: 10.3847/1538-4357/add0aa.
- V. Savchenko, C. Ferrigno, E. Kuulkers, and et al. *ApJL*, 848:L15, Oct. 2017. doi: 10.3847/2041-8213/aa8f94.
- F. K. Schinzel et al. *ApJL*, 876(1):L17, May 2019. doi: 10.3847/2041-8213/ab18f7.
- P. Scholz and Chime/Frb Collaboration. *The Astronomer's Telegram*, 13681:1, Apr. 2020.
- M. R. Schreiber et al. *Nature Astronomy*, 5:648–654, Apr. 2021. doi: 10.1038/s41550-021-01346-8.
- M. Serylak et al. *A&A*, 665:A53, Sept. 2022. doi: 10.1051/0004-6361/202142670.
- Z. Shi and C. Y. Ng. *ApJ*, 972(1):78, Sept. 2024. doi: 10.3847/1538-4357/ad5af8.
- X. Song et al. *MNRAS*, 505(3):4456–4467, Aug. 2021. doi: 10.1093/mnras/staa3805.
- A. Spitkovsky. *ApJL*, 648(1):L51–L54, Sept. 2006. doi: 10.1086/507518.
- I. H. Stairs, S. E. Thorsett, and Z. Arzoumanian. *Phys. Rev. L.*, 93(14):141101, Sept. 2004. doi: 10.1103/PhysRevLett.93.141101.
- A. G. Suvorov and A. Melatos. *MNRAS*, 520(1):1590–1600, Mar. 2023. doi: 10.1093/mnras/stad274.
- A. Szary, G. I. Melikidze, and J. Gil. *MNRAS*, 447(3):2295–2306, Mar. 2015. doi: 10.1093/mnras/stu2622.
- C. M. Tan et al. *ApJ*, 866(1):54, Oct. 2018. doi: 10.3847/1538-4357/aade88.
- T. M. Tauris and H.-T. Janka. *ApJL*, 886(1):L20, Nov. 2019. doi: 10.3847/2041-8213/ab5642.
- T. M. Tauris and E. P. J. van den Heuvel. *Physics of Binary Star Evolution. From Stars to X-ray Binaries and Gravitational Wave Sources*. Princeton University Press, 2023. doi: 10.48550/arXiv.2305.09388.
- T. M. Tauris, N. Langer, and M. Kramer. *MNRAS*, 425(3):1601–1627, Sept. 2012. doi: 10.1111/j.1365-2966.2012.21446.x.
- T. M. Tauris et al. In *Advancing Astrophysics with the Square Kilometre Array (AASKA14)*, page 39, Apr. 2015a. doi: 10.22323/1.215.0039.
- T. M. Tauris, N. Langer, and P. Podsiadlowski. *MNRAS*, 451(2):2123–2144, Aug. 2015b. doi: 10.1093/mnras/stv990.
- T. M. Tauris et al. *ApJ*, 846(2):170, Sept. 2017. doi: 10.3847/1538-4357/aa7e89.
- D. Thornton et al. *Science*, 341(6141):53–56, July 2013. doi: 10.1126/science.1236789.
- A. N. Timokhin. *MNRAS*, 408(1):L41–L45, Oct. 2010. doi: 10.1111/j.1745-3933.2010.00924.x.
- M. O. Toropov, S. A. Tyul'bashev, and V. S. Beskin. *Astronomy Reports*, 68(12):1191–1198, Dec. 2024. doi: 10.1134/S1063772924701026.
- J. D. Turner et al. *MNRAS*, 531(3):3579–3594, July 2024. doi: 10.1093/mnras/stae1300.
- J. D. Turner et al. *MNRAS*, 537(2):1070–1092, Feb. 2025. doi: 10.1093/mnras/staf098.
- V. Venkatraman Krishnan et al. *The Open Journal of Astrophysics*, 8:54246, Dec. 2025. doi: 10.33232/001c.154246.
- F. Verbunt and P. C. C. Freire. *A&A*, 561:A11, Jan. 2014. doi: 10.1051/0004-6361/201321177.
- F. Verbunt, A. Igoshev, and E. Cator. *A&A*, 608:A57, Dec. 2017. doi: 10.1051/0004-6361/201731518.
- D. Viganò et al. *MNRAS*, 434(1):123–141, Sept. 2013. doi: 10.1093/mnras/stt1008.
- D. Viganò et al. *Computer Physics Communications*, 265:108001, Aug. 2021. doi: 10.1016/j.cpc.2021.108001.

- G. Voisin et al. *A&A*, 638:A24, June 2020a. doi: 10.1051/0004-6361/202038104.
- G. Voisin et al. *MNRAS*, 499(2):1758–1768, Dec. 2020b. doi: 10.1093/mnras/staa2876.
- G. Voisin et al. *A&A*, 693:A143, Jan. 2025. doi: 10.1051/0004-6361/202452100.
- Z. Wang et al. *Nature*, 642(8068):583–586, June 2025. doi: 10.1038/s41586-025-09077-w.
- J. Yao et al. *Nature Astronomy*, 5:788–795, May 2021. doi: 10.1038/s41550-021-01360-w.
- J. M. Yao, R. N. Manchester, and N. Wang. *ApJ*, 835(1):29, Jan. 2017. doi: 10.3847/1538-4357/835/1/29.
- W. Yuan, C. Zhang, Y. Chen, and Z. Ling. The Einstein Probe Mission. In C. Bambi and A. Sanganello, editors, *Handbook of X-ray and Gamma-ray Astrophysics*, page 86. 2022. doi: 10.1007/978-981-16-4544-0_151-1.
- I. Yusifov and I. Küçük. *A&A*, 422:545–553, Aug. 2004. doi: 10.1051/0004-6361:20040152.
- B. Zhang, A. K. Harding, and A. G. Muslimov. *ApJL*, 531(2):L135–L138, Mar. 2000. doi: 10.1086/312542.
- L. Zhang et al. *arXiv e-prints*, art. arXiv:2512.17214, Dec. 2025. doi: 10.48550/arXiv.2512.17214.
- D. J. Zhou et al. *Research in Astronomy and Astrophysics*, 23(10):104001, Oct. 2023. doi: 10.1088/1674-4527/accc76.
- W. W. Zhu et al. *ApJ*, 734(1):44, June 2011. doi: 10.1088/0004-637X/734/1/44.